ENHANCED REMOVAL OF *Cryptosporidium*
OOCYSTS BY FILTER MEDIA COATED WITH HYDROUS IRON ALUMINUM
OXIDES

By

KATHRYN M. SHAW

A DISSERTATION PRESENTED TO THE GRADUATE SCHOOL
OF THE UNIVERSITY OF FLORIDA IN PARTIAL FULFILLMENT
OF THE REQUIREMENTS FOR THE DEGREE OF
DOCTOR OF PHILOSOPHY

UNIVERSITY OF FLORIDA

2001

To my mother and the three men of my life,
my husband, my father, and Nickolai.

TABLE OF CONTENTS

ENHANCED REMOVAL OF *Cryptosporidium* OOCYSTS
BY FILTER MEDIA COATED WITH HYDROUS IRON ALUMINUM OXIDES

By

Kathryn M. Shaw

August 2001

Chairman: Dr. Ben Koopman
Major Department: Department of Environmental Engineering Sciences

In the past 10 years, *Cryptosporidium* oocysts have been shown to be common

contaminants in water, causing at least 20 outbreaks of cryptosporidiosis affecting almost

500,000 individuals in the United States alone. Disinfection processes generally have

had limited success in removing *Cryptosporidium* from water. The success of

conventional filtration on the removal of *Cryptosporidium* oocysts is limited by filter

operating conditions and chemical conditioning.

A surface coating of hydrous aluminum and iron oxide on Ottawa sand was

investigated as a means of improving the removal of *Cryptosporidium* oocysts from water

by filtration. Coating the sand increased the zeta potential from -40 mV to +45 mV at pH

7.0, enhancing the potential for interaction with the negatively charged (-25 mV at pH

7.0) *Cryptosporidium* oocysts. Water seeded with *Cryptosporidium* oocysts was passed

through parallel columns of uncoated and coated sand at superficial velocities of 200 to

vi

800 m/d (3.5 to 14 gal/(ft^2 min)) and column lengths of 10 to 40 cm (4 to 16 in.). In every trial, removals of the oocysts with coated sand were significantly higher than removals with uncoated sand. Filter coefficients of coated sand were 2.9 times higher than those of uncoated sand, indicating that performance of granular media filters for *Cryptosporidium* removal can be significantly enhanced by the coating technology.

Iron aluminum (hydr)oxide was coated on glass and ceramic beads by *in situ* precipitation from metal chloride solutions, followed by contact with ammonium hydroxide. Zeta potential at pH 6 to 8 of glass beads was increased from negative to positive values by the coating, whereas zeta potential of ceramic beads was positive both before and after coating. Removal of *Cryptosporidium* oocysts in batch tests and continuous-flow column tests was significantly improved by coatings on both types of beads. These results show that, while electropositive character is the most important factor in design of coatings for granular media to enhance filtration of *Cryptosporidium*, other factors (e.g., affect of coating on surface area and surface roughness of filter media) should also be considered.

Waterborne diseases are a danger to public health in the United States and around the world. The presence of *Cryptosporidium* oocysts in water supplies is currently a significant public health concern because of the association of the microbes with surface runoff, and because of their role in several large outbreaks of gastroenteritis. In the past several years, *Cryptosporidium* has been responsible for at least 20 outbreaks of cryptosporidiosis affecting approximately 500,000 individuals in the United States alone (Rose, 1998).

Disinfection is a water treatment process commonly used to prevent microbes from contaminating drinking water. Although the use of disinfection has greatly reduced the number of outbreaks of some waterborne illnesses, it has had limited success in the inactivation of some waterborne pathogens, such as *Cryptosporidium* oocysts. One U.S. study (Fayer et al., 1996) found that 90% of a sample of *Cryptosporidium* oocysts were still viable after spending 2 hours in undiluted household bleach. Since disinfection is not a reliable barrier to *Crypstosporidium* contamination, physical removal of the oocysts is necessary.

Filtration is a process used to prevent microbial contamination of drinking water. Several studies (Fogel et al., 1993; Ongerth and Pecoraro, 1995; Schuler et al., 1991; Whitmore and Carrington, 1993) have examined the effectiveness of sand filtration of *Cryptosporidium* oocysts. They show that the success of conventional filtration in the removal of *Cryptosporidium* oocysts from water is highly dependent upon (and often

1

limited by) filter operating conditions and chemical conditioning of the water. The development of a method of increasing the reliability of sand filtration for the removal of *Cryptosporidium* oocysts is needed.

Studies show that coatings of metallic hydroxides, oxides, and peroxides on filter media enhance the removal of bacteria, viruses, and turbidity from water and wastewater (Ahammed and Chaudhuri, 1996; Chang et al., 1997; Chen et al., 1998; Farrah and Preston, 1991; Gerba et al., 1988; Lukasik et al., 1996; Lukasik et al.,1999; Mills et al., 1994; Shaw et al., 2000; Stenkamp and Benjamin, 1994). The filter media, which are electronegative in their natural state, become electropositive as a result of the coating process. Since the particles are electronegative in the natural water pH range of 6 to 9, the enhanced removal has been attributed to a decrease in electrostatic repulsion between the particles and the coated filter media.

The size of microbes in previous studies of filter media surface modification ranged from 0.5 to 2.0 µm for bacteria, down to 40 to 60 nm for viruses. *Cryptosporidium* oocysts cover a size range of 4 to 8 µm (Levine, 1984). Filter media coating technology, to be commercially viable for water purification, must be shown to be effective against particles in this size range also. Along with size differences, other factors, such as surface composition, surface characteristics and diffusivity in water can influence the removal of *Cryptosporidium* oocysts from water. The first phase of this study examines the effectiveness of the iron aluminum (hydr)oxide coating on Ottawa sand for the removal of *Cryptosporidium* oocysts.

A few investigators have cited other changes in the filter media as a result of the coating process as contributing factors in enhanced particle removal. Factors include surface area and surface roughness, surface chemical heterogeneity, and amphoteric

surface charge (Stenkamp and Benjamin, 1994; Sansalone, 1999) Long-term studies show that the electropositive surface of the filter media can revert back to electronegative in time and still remove significantly more microbes than uncoated media (Chen et al., 1998). Thus, other changes in the characteristics of the filter media surface due to coating must also play a role in enhancing filtration performance. The second phase of this study examined the effect of changing the zeta potential of the filter media on the removal of *Cryptosporidium* oocysts from water.

The following specific objectives were chosen for this study because of knowledge gaps revealed above:

1. Evaluate the aluminum and iron (hydr)oxide coating on filter media in terms of its ability to enhance the removal of *Cryptosporidium* oocysts using varied column lengths and superficial velocities.

2. Quantify the non-electrostatic contribution of iron aluminum (hydr)oxide coating on granular filter media (glass and ceramic beads) to removal of *Cryptosporidium* oocysts.

2-1 *Cryptosporidium*

2-1-1 General

Cryptosporidium is a genus of 21 known species of enteric coccidian protozoans. It was first described in 1907 by E.E. Tyzzer (Rose, 1990). The organism was isolated from gastric mucosa in the stomach of a laboratory mouse, and named *C. muris*. Four years later, a second species that inhabited the small intestine of the mouse, was identified (Tyzzer, 1910; Tyzzer, 1912). This species was named *C. parvum*.

In 1955, *Cryptosporidium* was discovered as a source of disease in agricultural animals. It was described during an outbreak of diarrhea in a domestic turkey flock (Slavin, 1955), and in 1971, *Cryptosporidium* was found to be the source of diarrhea in a herd of dairy cows (Panciera et al., 1971). Many studies over the next 10 years found that *Cryptosporidium* was a significant cause of illness, and often mortality, in calves and lambs (Anderson et al., 1982, Angus et al., 1982, and Current et al., 1983).

Cryptosporidium was not recognized as a source of human illness until 1976. At this time, an infection was found in an immunocompromised individual (Meisel et al., 1976) and an apparently otherwise healthy 3-year-old (Nime et al., 1976). Since then, reports of cryptosporidiosis in humans have increased. Most infections were found in patients with compromised immune systems (Navin and Juranek, 1984). As the prevalence of Acquired Immune Deficiency Syndrome (AIDS) increased, *Cryptosporidium* was shown to be a causative agent in diarrhea in AIDS patients. Since infection by *Cryptosporidium*

4

was suspected as a major cause of death in these patients, with mortality rates as high as 50% (Rose, 1990), it became critical to develop a rapid diagnostic test and treatment.

Although there are several therapeutic agents currently being investigated (Upton, 1997; Woods and Upton, 1998), none have yet been found to be effective. However, the diagnosis of infection by oocyst detection in feces in lieu of intestinal biopsies was a major advancement (Current et al., 1983).

Cryptosporidium undergoes a life cycle similar to that of most coccidia (Current and Garcia, 1991; Fayer and Unger, 1986; Long, 1982). The infective stage of the disease is the oocyst and the infective dose, generally reported as 10 to 100 oocysts, may be as low as a single oocyst (Meinhardt et al., 1996). The oocyst, which is resistant to most environmental conditions, is released by one host and ingested by its new host. As shown in Figure 2-1, after ingestion occurs, the oocyst undergoes excystation, releasing the sporozoites. The sporozoites initiate the infection within the epithelial cells of the gastrointestinal tract. The sporozoite then differentiates into the trophozoite which undergoes asexual multiplication to form Type I meronts and then merozoites which may infect new host cells. Merozoites from Type II meronts produce microgamocytes and macrogamocytes that undergo sexual reproduction to form the oocyst. The infected individual excretes oocysts in the feces, and the oocysts are infective immediately.

The oocyst is a spherical particle with a diameter of 4 to 8 microns (Levine, 1984). The DNA sequencing of *Cryptosporidium* oocysts' surface proteins suggests a surface-adherent molecule, rich in cysteine, proline and histidine and capable of forming disulfide bonds (Tilley and Upton, 1997). However, other studies have shown that the outer wall of *Cryptosporidium parvum* oocysts contains galactase/galactosamine and glucose/gluco-
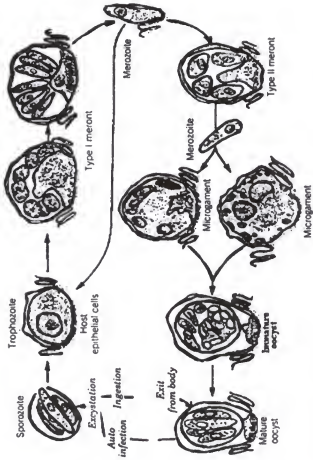
Figure 2-1. Life Cycle of *Cryptosporidium* (Fayer and Unger, 1986)

samine residues, possibly with both N- and O-linked glycosylation (Considine et al., 2000).

2-1-2 Public Health Perspective

Cryptosporidium is one of the primary causes of waterborne illness (Rose, 1990). It is the most predominant intestinal protozoan, ranking sixth behind the enteric bacteria (Marshall et al., 1987), and the most predominant parasite infection (Holly and Dover, 1987). In one incident alone, over 403,000 individuals became ill in an outbreak of cryptosporidiosis in Milwaukee, Wisconsin. This incident was judged to cost the community some $53 million in lost wages, lost productivity, medical bills and emergency room visits, as well as $100 million in claims of loss of life (Smith and Rose, 1998). Between 250 and 500 million infections of *C. parvum* are reported to occur annually in Asia, Africa, and Latin America (Current and Garcia, 1991).

2-1-3 Filtration of *Cryptosporidium*

Several researchers investigated the effectiveness of sand filtration for the removing *Cryptosporidium* oocysts from water. These studies are shown in Table 2-1. Ongerth and Pecoraro (1995) investigated the effect of optimization of chemical conditioning on the removal of *Cryptosporidium* oocysts. Near-complete removal was achieved under optimum conditions. However, when conditions were allowed to drop below optimum levels, removals decreased. Whitmore et al. (1993) studied the effect of hydraulic loading on the removal of *Cryptosporidum*. As hydraulic loading increased, removals decreased. At a hydraulic loading of 5 m/h, a conservative loading for a rapid sand filter, the removal rate of *Cryptosporidium* is quite low.

Table 2-1. Sand Filtration of *Cryptosporidium* oocysts.

Sand Size, mm (in.)	Bed Depth, m (ft)	Hydraulic Loading, m/h (gal/(ft² min))	Chemical Conditioning	Removal	Study
0.27 (0.01)	0.90 (2.95)	0.15-0.4 (0.0001-0.0003)	None	>99.99%	Pilot Scale (Schuler, 1991)
0.2-0.3 (0.008-0.012)	1.05 (3.44)	0.19-0.4 (0.0001-0.0003)	None	48%	Full Scale (Fogel, 1993)
0.45-0.55 (0.018-0.022)	1.2 (3.94)	12.2 (0.009)	Alum Coagulation Optimum Conditions Suboptimum Conditions	>99.8% 96%	Pilot Scale (Ongerth and Pecoraro, 1995)
0.58-0.63 (0.023-0.025)	1.0 (3.28)	0.1-0.4 (0.00007-0.0003) 1.0-19.8 (0.0007-0.0.01)	None None	97.3-98.4% 2.3-43.2%	Lab Scale (Whitmore, 1993)

2-2   Microbial Attachment to Surfaces

Removal of *Cryptosporidium* oocysts and other microbes from water by filtration depends on the ability of the microbes to attach to the surface of the filter media. Adhesion of particles to surfaces involves several processes, as shown in Figure 2-2. Transport of the particle to the surface results from body forces, such as gravitational forces (sedimentation); hydrodynamic forces (fluid flow) causing movement of the particle; or, in the case of microbes, the cell's own mobility. As the particle gets closer to the surface and approaches the diffusive boundary layer, fluid convection in the direction normal to the surface becomes negligible. At these shorter distances, the particle can be transported by Brownian motion resulting from thermal fluctuations in the surrounding fluid. The next step is the attachment of the particle to the surface. This is accomplished by longer range forces (> 5 nm); namely van der Waals forces, electrostatic interactions, and the influence of macromolecules on the cell surface. Adhesion of the particle to the surface requires that the particle resist detachment. Detachment is governed by shorter range forces (< 5 nm), specifically, shorter range van der Waals forces, electrostatic interactions and hydrogen bonding.

2-2-1   Electrostatic Interactions

All solid surfaces in an aqueous medium carry a surface charge. The surface charge is a result of either the ionization of surface groups or the adsorption of ions from the solution. A charged surface then attracts ions of the opposite charge. The counter ions can be closely associated with the surface or distributed exponentially into the solution. When two solid surfaces approach each other, the surfaces with like charges
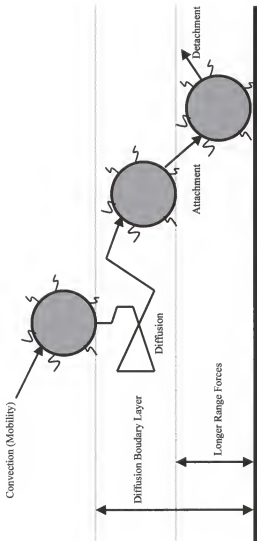
Figure 2-2. Microbial adhesion as a sequence of dynamic processes. (Dickinson et al., 2000)

experience repulsion when their electrical double layers overlap. Solid surfaces with opposite charges attract each other.

2-2-2 Van der Waals Forces

A molecule, even a nonpolar one, can have a momentary unequal distribution of electron density. There can be an excess of electron density in one region of the molecule and a corresponding deficiency in another area. An uneven distribution of electron density can create an instantaneous dipole, and the instantaneous dipole can create a dipole in a second non-polar molecule, creating an attraction. These weak interactions are collectively called van der Waals forces.

2-2-3 DLVO theory

Derjaguin and Landau (1941) and Verwey and Overbeek (1948) proposed that the total interaction force between surfaces was the additive combination of van der Waals attraction and electrostatic repulsion. Figure 2-3 shows a plot of the energy of interaction of two surfaces as a function of their separation distance. The bottom line on this plot represents the van der Waals attraction. This is a negative term which is an inverse power law function of separation. The top line on this plot represents the double layer interactions. This is a positive term which decreases exponentially as separation distance increases. The net energy of interaction (represented by the middle line) is the sum of the van der Waals and electrical double layer interactions.

Two minimums are apparent on the line representing the sum of the two interaction forces. The minimum occurring at the shorter separation distance, the primary minimum, corresponds to a balance between the short-range repulsive forces and attractive forces. This minimum is present at low or high electrolyte concentration. When a particle comes into this region of the graph, it will be pulled to the surface and
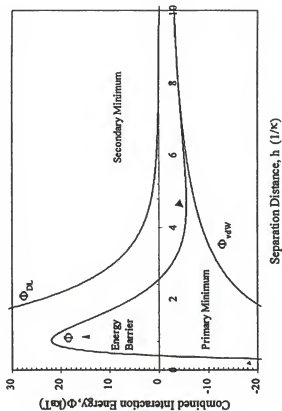
Figure 2-3. Hypothetical DLVO energy potential curve.

permanently attached to it. A secondary minimum at a greater separation distance corresponds to a balance between long-range attractive and repulsive forces. The minimum is present only at high electrolyte concentration, because the double layer term decays more sharply, allowing the van der Waals term to remain significant at a separation distance beyond the range of repulsion. The particles can remain in this secondary minimum, and it results in a much weaker adhesion. The attachment, in this case, could be reversed by shear or reducing the salt concentration. Because interaction potentials are directly proportional to particle size, secondary minimum effect is more significant with larger particles (greater than 1 micron in diameter, Elimelech et al., 1995).

As previously mentioned, the interaction energy between a charged particle and a charged surface predicted by DLVO theory is the sum of the electrical double layer contribution and the van der Waals contribution. Quantitative prediction of these contributions involves measurements such as zeta potential, dielectric constant and Hamaker constant, which are briefly explained below.

2-2-3-1 Zeta potential

Double layer interactions are generally quantified by the zeta potential. Surface potential is an important factor in microbial adhesion. Surface potential can be approximated by zeta potential or surface charge. In the case of microbial adhesion, it is often assumed that the surface potential is constant over the entire surface of the microbe even though the surface of cells is not homogeneous. Surface charge refers to the charge character of the surface due to its actual molecular composition. Zeta potential is the potential resulting from that charge at a particular distance from the surface. The distance is the plane of shear. At this plane, the ion association of the surrounding

solution (the electrical double layer) can reduce the magnitude of the charge slightly. However, when the electrolyte solution is dilute, the number of these associating ions which shield the surface charge is minimized. In this case, the zeta potential can be assumed to equal the surface potential.

2-2-3-2 Hamaker constant

Van der Waals attraction is evaluated by two methods. One approach is microscopic (Hamaker, 1937): the total interaction between two particles is found by a pairwise summation of all of the relevant intermolecular interactions. The resulting expressions can be split into a purely geometric element, and the Hamaker constant. The Hamaker constant is related only to the properties of the particles and the medium. It is a function of the number of atoms per unit volume of particles and the London dispersion force constant that is related to the polarizability of the molecule.

2-2-3-3 Dielectric constant

The second method, suggested by Liftshitz (1956), is a macroscopic approach for evaluating the van der Waals force. If a polar substance is placed in an electric field, its molecules become oriented so that their positive ends face the negative pole and the negative ends face the positive pole. This alignment partially neutralizes the field. The dielectric constant of a substance is a measure of the extent to which the field is neutralized. Dielectric measurements are taken as a function of frequency. The attraction between two materials in a particular medium is related to the summation of the dielectric spectra between the materials and the media.

2-2-4 Non-DLVO Interactions

Since the development of DLVO theory, many researchers have obtained experimental results that could not be explained by DLVO theory. As a result, several

other interactions have been proposed to explain these results. The additional interactions include hydration forces, hydrophobic forces and macromolecule-induced forces.

2-2-4-1 Hydration force

One of the non-DLVO interactions that was proposed is the hydration force (Israelachvili, 1992). Ionic groups or hydrophilic sites on a surface can cause water to be bound tightly to that surface. If the particle is hydrated in this manner or the collector surface is hydrated, an extra repulsion to attachment can occur. The extra repulsion occurs because the surfaces must become dehydrated to allow the particle and collector surfaces to make contact with each other.

2-2-4-2 Hydrophobic forces

An additional non-DLVO interaction is hydrophobic interactions (Stenstrom, 1989; van Loosdrecht et al., 1987a; van Loosdrecht et al., 1987b; Gerba et al., 1988). When a surface has no polar or ionic groups or hydrogen-bonding sites, it is hydrophobic. When two hydrophobic surfaces are brought together, there is an attraction. Hydrogen bonding between the molecules in bulk water cause it to be more structured than water that is in contact with a hydrophobic surface. As a result, the free energy of water in the gap between hydrophobic surfaces increases as the distance between the surfaces decreases, and the water tends to leave the gap.

2-2-4-3 Macromolecule-induced forces

Macromolecules present in the gap between a particle and a collector surface can affect the attachment of the particle to the surface (Dickinson, 1997). Polymeric molecules can adsorb on the surface of a particle or collector. When only a small amount of polymer is present, it can adsorb on more than one surface, causing a bridging effect.

When a larger amount of polymer is present and the surfaces of the particle and collector are coated, the polymer layers can overlap and cause steric repulsion. The repulsion is a result of the need for the hydrophilic chains to become dehydrated to allow the polymer layers to overlap.

EFFECT OF HYDROUS IRON ALUMINUM OXIDE COATING ON SAND IN
THE FILTRATION OF *Cryptosporidium* OOCYSTS

3-1 Introduction

The presence of *Cryptosporidium* in water supplies is a widespread problem in the

U.S. and other nations. This protozoan causes severe gastroenteritis which is potentially

fatal to infants and immunocompromised individuals and which does not respond well to

available therapeutics. Rose (1998) found that 77% of rivers and 75% of the lakes

sampled in a U.S. survey had detectable levels of *Cryptosporidium*. Also, 83% of

pristine waters (with no human activity in the watershed) and 28% of the treated drinking

water samples had detectable levels of *Cryptosporidium* oocysts. In the U.S., over

431,000 confirmed cases of cryptosporidiosis have been reported since the disease was

identified in 1976 (Rose, 1998). Most (403,000) of these cases are from the 1993

outbreak in Milwaukee, Wisconsin. Between 250 and 500 million infections occur

annually in Asia, Africa, and Latin America (Current and Garcia, 1991). Recently, 1100

cases of cryptosporidiosis were reported in Sydney, Australia.

The infective stage of the disease is the oocyst and the infective dose, generally

reported as 10 to 100 oocysts, may be as low as a single oocyst (Meinhardt et al., 1996).

The oocysts are resistant to disinfectants and most environmental conditions, thus making

physical removal by treatment processes necessary. Chemical conditioning and optimum

operation of filtration systems can achieve greater than 99% removal of oocysts from

water (Ongerth and Pecoraro, 1995; Schuler et al., 1991). Suboptimal flocculation can

17

lead to substantially decreased performance, however, dropping the removal to 96% at a superficial velocity of 293 m/d (Ongerth and Pecoraro, 1995). Fogel et al.(1993) obtained removals of only 2 to 43% at hydraulic loads of 24 to 475 m/d when chemical conditioning was not practiced.

Cryptosporidium oocysts carry a negative surface electrical charge in the pH range of natural waters (Drozd and Schwartzbrod, 1996; Karaman et al., 1999; Ongerth and Pecoraro, 1996), whereas natural filter media such as sand and diatomaceous earth also carry a negative surface electrical charge in this pH range (Chen et al., 1998; Farrah and Preston, 1991). Thus, removal of the oocysts particles by filtration (without chemical conditioning) will be difficult due to electrostatic repulsion between the oocysts and the filter media surface. Coatings of metallic hydroxides, oxides, and peroxides on filter media have been found to enhance the removal of bacteria, viruses, and turbidity from water and wastewater (Ahammed and Chaudhuri, 1996; Farrah et al., 1991, Gerba et al., 1988; Mills et al., 1994, Lukasik et al., 1996). However, no studies have been carried out to determine if the application of electropositive coatings to granular filtration media can improve removal of *Cryptosporidium*. Extrapolation of results from previous studies with bacteria and viruses is problematical, since the oocysts, which are 5 to 7 μm in diameter, are significantly larger than the microbes tested previously. The purpose of the present study was therefore to determine the effect of coating filter media (Ottawa sand) with hydrous aluminum iron oxide on removal of *Cryptosporidium*. Performance of coated and uncoated sand was investigated over ranges of superficial velocity and filter column length.

3-2 Materials and Methods

3-2-1 Coating Method

The fraction of 20 x 30 mesh Ottawa sand (Fisher Scientific) passing a U.S. Standard #25 sieve was collected to obtain particles between 0.6 and 0.7 mm in diameter. The sieved sand was filled to a depth of 2.5 cm in flat plastic pans, then covered with a solution 0.4 M in $AlCl_3 \cdot 6H_2O$ and 0.2 M in $FeCl_3 \cdot 6H_2O$ (Fisher Scientific). The solution was immediately drained from the sand, and the sand was dried at 70° C for 24 h, then cooled to room temperature. Clumps in the dried sand were broken up, then the sand was poured into a beaker containing 4 M ammonium hydroxide (Fisher Scientific). The solution was immediately drained from the sand, then the sand was spread over flat pans, dried at 70° C for 24 h, and cooled. The dried sand was re-sieved using a #25 screen, rinsed with deionized water until the water was clear, air-dried, and stored in sealed plastic containers until use.

To measure iron and aluminum contents, 10.0 g of oven-dried (105° C) sand was digested in 25.0 mL of gently boiling aqua regia (1:2:2 $HCl:HNO_3:H_2O$) for 20 min. After cooling, the digestate and water from rinsings of the digestion vial and sand were passed through Whatman GF/C filters, and the final volume was made up to 100 mL. This solution was analyzed for aluminum and iron by ICP.

3-2-2 Sand Columns

Dry sand was packed into 1.5 cm I.D. acrylic columns of varying lengths, depending on the experiment. Sand quantities were 39 g in the 10 cm columns, 78 g in the 20 cm columns, 114 g in the 30 cm columns, and 154 g in the 40 cm columns. Glass wool was

used at both ends of the columns to prevent loss of filter media. Columns were used in the upflow mode.

Columns containing uncoated sand and coated sand were run in parallel in each trial and were fed artificial groundwater (AGW) containing 35 mg $MgSO_4 \cdot 7H_2O$, 12 mg $CaSO_4 \cdot 2H_2O$, 12 mg $NaHCO_3$, 6 mg $NaCl$, and 6 mg KNO_3 per liter deionized water (McCaulou et al., 1994) with a pH of 7.0. Immediately prior to each experiment, packed columns were rinsed with 70 pore volumes of AGW at the same flow rate used in the experiment. *Cryptosporidium* oocysts (Pleasant Hill Farms, Troy, Idaho) were added to 20 to 70 L of AGW in a plastic container to give approximately 500 to 1000 oocysts/mL. The AGW was mixed at 60 rev/min with a 5 cm diameter propeller-type impeller throughout the experiments. Influent to the columns was sampled from the container while pore volumes 71 to 75 were entering the columns. Composite effluent samples representing steady state conditions were collected at the 71st through 75th pore volumes. Samples were then refrigerated overnight prior to enumeration. Three trials were carried out for each column length and superficial velocity tested.

3-2-3 Counting of *Cryptosporidium* Oocysts

The fluorescent antibody method of EPA (1995) was used in enumerating the *Cryptosporidium* oocysts. The waters tested were reconstituted in the laboratory and the oocysts were added from commercial sources, therefore the positive identification step involving visualization of internal structures of the oocysts was omitted. For each sample, one slide was prepared for the influent and one slide was prepared for the effluent.

Reagents used in enumerating *Cryptosporidium* oocysts included phosphate buffered saline (PBS), blocking solution, fluorescent reagent, and mounting medium. The PBS

(Sigma) had a pH of 7.6. Blocking solution was composed of 1% bovine serum albumin (BSA), 10% normal goat serum (NGS), and 0.02% thimerosol in PBS (reagents from Sigma.) The blocking solution was prepared by combining 10 mL NGS and 90 mL PBS, then placing 1 g BSA and 0.02 g thimersol (both in powder form) on the liquid surface. The powders were allowed to dissolve before mixing the solution. Blocking solution was made up weekly. Mounting medium was prepared by mixing together 90 mL glycerol, 10 mL PBS, and 2 g of 1,4-diazabicyclo(2,2,2)octane (reagents from Sigma). The fluorescent reagent was prepared with a Crypt-A-Glo kit (Waterborne, New Orleans, LA). The kit contains 5-carboxy-fluorescein-labeled IgM monoclonal antibody made against oocysts of *Cryptosporidium parvum*. The working dilution was obtained by adding 0.25 mL of the antibody reagent to 5 mL of blocking solution, followed by gentle stirring. The working dilution was prepared fresh for each assay.

Filters were soaked in PBS for 2 min. A wet support filter (0.45 μm effective pore size; Gelman GN6) was placed on each support screen of the vacuum manifold (Hoefer model FH 225V) and a cellulose acetate filter (0.2 μm effective pore size cellulose acetate; Sartorius, Edgewood, N.Y.) was placed atop each support filter. The vacuum was adjusted to 5 to 10 cm Hg, then a manifold valve was opened briefly to flatten the filter. (Valves were opened only long enough to drain liquids, in order to avoid drying the filters.) The filter was rinsed with 2 mL of blocking solution to limit non-specific background fluorescence. A 5 mL volume of sample was then passed through the filter, followed by an additional rinse of 2 mL of blocking solution. A volume of 0.5 mL fluorescent reagent was placed on the filter and left for 45 minutes. Light was excluded during the contact period by covering the filter funnel with aluminum foil. After draining the fluorescent reagent, the filter was rinsed 5 times with 2 mL PBS per rinse.

The slide was prepared by placing a 75 μL drop of mounting medium on a slide and warming the slide to 37 ° C. A single filter was placed atop the mounting medium on a slide, completely wetting the bottom of the filter. A 25 μL drop of mounting medium was added to the top of the filter. Finally, a glass cover slip was placed over the filter and weighted with 5g of coins to flatten the filter. The edges of the cover slip were sealed with quick drying nail enamel.

The 5 to 7 micron diameter *Cryptosporidium* oocysts appeared apple-green and spherical with a darker green outline under epifluoresence illumination (Leitz Microlab with 25x bright field objective and 12x ocular). The entire slide was counted. Since the filtered suspension was in reconstituted water, very little debris was visible on the prepared slides. Typical influent counts per slide were approximately 2000 oocysts, compared to effluent counts of 5 to 800 oocysts.

3-2-4 Zeta Potential Measurements

The zeta potential of the *Cryptosporidium* oocysts was measured over a pH range of 5 through 8 using a Brookhaven Zeta Plus. The oocysts were purchased without a preservative (i.e. in deionized water only). The pH was adjusted using NaOH and HCl (Fisher Scientific). Each sample was adjusted to 0.001 M NaCl. The *Cryptosporidium* oocyst mass concentration used was approximately 0.05 mg/mL . The electrode was cleaned by sonicating for 5 to 10 minutes every 3 to 4 runs.

The zeta potential of the uncoated and coated sand was determined using a streaming potential apparatus consisting of a flow cell packed with the granular filter media, a reservoir of electrolyte (1.0×10^{-3} M KCl) for the flow cell, electrodes and a voltmeter (ExTech 380282) to measure the potential difference across the flow cell, and manometer to measure the pressure drop across the flow cell. The flow cell was made

from clear acrylic tubing with a length of 50 cm and an inner diameter of 3.8 cm. The electrodes were located at the two ends of the flow cell and were formed from fine silver mesh was cut to match the cross section of the flow cell. Silver wire (18 gauge) was spot welded to the center of each electrode. The electrodes were anodized in HCl for 30 to 60 minutes using a copper or platinum cathode and a 10 mA current. The electrodes were re-plated periodically to ensure proper performance.

Sand samples were uniformly packed into the sample cell via the tap and fill methodology. The sample cell was flushed with the KCl electrolyte solution to remove air pockets. Single trials were carried out over a range of pressure drops and corresponding potential differences in order to find the ratio of streaming potential (E_{str}) to pressure drop through the media (p) for a given pH and sand type. This ratio was used to find zeta potential (ζ) according to the equation (Hiemenz and Rajagopalan, 1997):

$$\zeta = \left(\frac{E_{str}}{p} \right) \frac{\eta k}{\varepsilon} \tag{3.1}$$

where η is the viscosity of water and k is conductivity. The parameter ε in SI units is found from:

$$\varepsilon = \varepsilon_r \, \varepsilon_0 \tag{3.2}$$

where $\varepsilon_r = 78.54$ at 25°C and $\varepsilon_0 = 8.85 \times 10^{-12}$ C^2/(J m).

3-3 Results and Discussion

3-3-1 Physical Characterization of *Cryptosporidium* and Sand

The SEM image in Figure 3-1 shows the spherical shape of a typical *Cryptosporidium parvum* oocyst. Due to shrinkage in preparation, the oocyst imaged is

Figure 3-1. Scanning electron micrograph of *Cryptosporidium parvum* oocyst (30,000x)

smaller than the typical 5 to 7 μm diameter as determined by epifluorescence microscopy (Rose, 1998). Zeta potential of *Cryptosporidium* oocysts in 10^{-3} KCl was negative over the pH range 5 to 8, in agreement with other investigators (Drozd and Schwartzbrod, 1996; Karaman et al., 1999; Ongerth and Pecoraro, 1996). Our measured values ranged from -17 mV at pH 5 to -29 mV at pH 8 (Fig. 3-2). These are in excellent agreement with the relationship given by Drozd and Schwartzbrod (1996), but are somewhat more electropositive than values given by Ongerth and Pecoraro (1996) and Karaman et al. (1999).

At 30x, uncoated and coated grains of Ottawa sand were indistinguishable (Fig. 3-3a). At 2000x, the morphology of coated sand was still essentially the same as the uncoated sand (Fig. 3-3b). Zeta potential of uncoated sand ranged from 0 mV at pH 2.6 to -55 mV at pH 10.7 (Fig. 3-4). The isoelectric point of uncoated sand (pH 2.5) is consistent with the value of pH 2 to 3 given by Parks (1965) for the α-quartz form of SiO_2. Coating the sand with aluminum and iron hydoxy(oxides) made the zeta potential more electropositive (Fig. 3-4). The isoelectric point of the coated sand was 8.0, which is between the range of 4.8 to 6.8 for iron oxides (Fe_2O_3 - haematite; FeOOH - goethite) and 7.8 to 9.1 for aluminum oxides (Al_2O_3 - corundum; AlOOH - boehmite) as given by Parks (1965).

The uncoated Ottawa sand had an iron content of 0.11 ± 0.026 mg/g sand and an aluminum content of 0.014 ± 0.003 mg/g sand (Table 3-1). Coating the sand increased the iron content to 1.36 ± 0.11 mg/g sand and the aluminum content to 1.22 ± 0.081 mg/g sand. These iron contents fall within the range of values reported by others (Edwards and
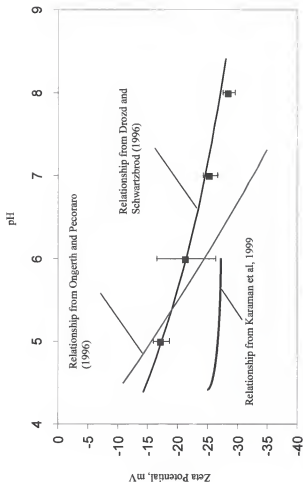
Figure 3-2. Zeta potential of *Cryptosporidium* oocysts in relation to pH. (Data points from present study; Error bars represent ± 1.0 standard deviations. The line for Drozd and Schwartzbrod (1996) was plotted from the equation in Figure 5 of their paper; the lines for Ongerth and Pecoraro (1996) and Karaman et al. (1999) are visual fits to their data.

b.

a.
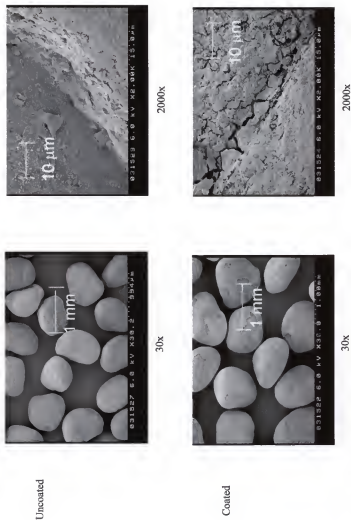
Uncoated

Coated

Figure 3-3. Scanning electron micrographs of Ottawa sand before and after coating (a) magnified 30x and (b) magnified 2000x.
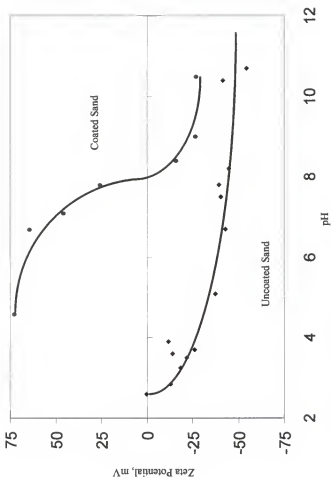
Figure 3-4. Comparison of zeta potential of uncoated sand to the zeta potential of sand coated with iron / aluminum (hydroxy)oxide

Table 3-1. Iron and aluminum contents of uncoated and coated sand.

Sand size mm (in.)	Fe, mg/g sand	Al, mg/g sand	Reference
0.6-0.7 (0.02-0.03) (Uncoated)	0.11	0.01	Present study
0.6-0.7 (0.02-0.03) (Coated)	1.7	1.2	
0.6-0.8 (0.02-0.04)	0.7	- -	Edwards and Benjamin (1989)
0.6-0.7 (0.02-0.03)	- -	0.4	Chen et al. (1998)
1.1 (0.04) (effective size)	1.6	0.8	Kang (1998)
0.7-1.2 (0.03-0.05)	1-2	- -	Lo et al. (1997)
"Fines"	0.6-0.7	- -	Stahl and James (1991)

Benjamin, 1989; Kang, 1998; Lo et al., 1997; Stahl and James, 1991), whereas the aluminum contents are somewhat higher than values previously reported (Chen et al., 1998; Kang, 1998). The Al/Fe molar ratio in the coating was 2:1 in the present study, compared to 1:1 in the coating solution. The enrichment for aluminum may be because the aluminum coating binds better to the sand. Truesdail (1999) found that attrition rates for iron hydroxide coatings were significantly higher than for aluminum hydroxide coatings. In our work, the rinsing and handling as part of the preparation procedure could cause loss of iron.

3-3-2 Attainment of Pseudo-Steady-State in Filtration Experiments

Pseudo-steady-state conditions were obtained shortly after starting the filter runs. This is demonstrated in Figure 3-5, which shows that the performance of filters using either coated sand or uncoated sand did not vary in relation to the length of the filtration period up to a filter run length of 420 minutes [782 pore volumes at a superficial velocity (U) of 407 m/d]. Lines representing least squares linear fits to the data for both coated and uncoated sand had slopes that were not statistically different from zero ($P < 0.05$). A long-term experiment with uncoated sand (Fig. 3-6) showed that pseudo-steady-state conditions were maintained for at least 30 hours (5000 pore volumes at $U = 81$ m/d). Based on an influent concentration of 272 oocysts/mL, an average removal of 97%, 6-μm diameter oocysts, and 0.65 mm spherical sand particles, the surface coverage of sand by the *Cryptosporidium* was estimated to be 3% at the end of the 30-h period. This degree of surface coverage is evidently too small to affect the rate of attachment of the oocysts to the sand.

Because the superficial velocities varied depending on the experiment, the appropriate sampling time was defined in terms of the number of pore volumes
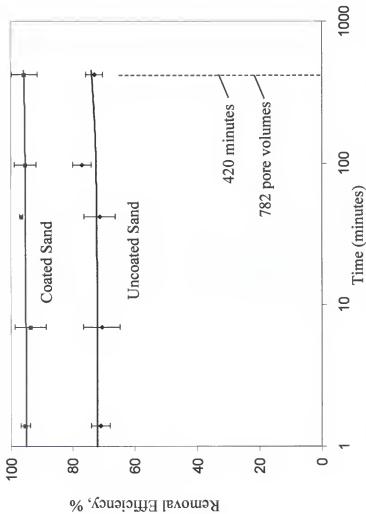
Figure 3-5. Effect of column run time on *Cryptosporidium* removal efficiency in sand columns (U = 407 m/d, L = 40 cm ; Error bars represent ± 1.0 S.D.)
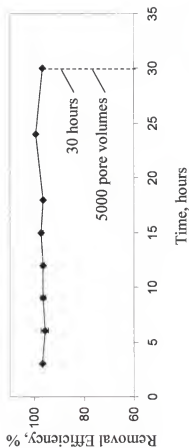
Figure 3-6. Effect of extended column run-time on *Cryptosporidium* removal efficiency (U = 82 m/d, L = 5 cm ; Error bars represent ± 1.0 S.D.)

processed. Comparisons of pseudo-steady-state filter performance were made using samples of the 70th through 75th pore volumes leaving the filter. These were well within the pseudo-steady-state region of filter performance.

3-3-3 Effect of Coating on Filtration Performance

The change in the concentration of particles with respect to column length in a granular media filter can be modeled by the first-order relation

$$\frac{\partial c}{\partial z} = -\lambda c \tag{3.3}$$

where c is the particle concentration at length z and and λ is a coefficient that characterizes the filter media. Under conditions in which the coverage of filter media by particles is low enough so that it does not affect the rate of particle attachment, the above expression may be integrated over the length of the filter column, yielding

$$\frac{c_{effl}}{c_{in}} = e^{-\lambda L} \tag{3.4}$$

where c_{in} = influent concentration of particles and c_{effl} = effluent concentration of particles. Equation (3-4) can be combined with the definition of fractional removal efficiency ($\eta = 1 - c_{effl}/c_{in}$) to obtain

$$\eta = 1 - e^{-\lambda L} \tag{3.5}$$

Equation (3-5) indicates that, as the filter coefficient increases, the removal efficiency for a given column length also increases. Figure 3-7 shows least squares nonlinear fits of Equation (3-5) to removal fraction vs. column data for uncoated sand and coated sand loaded at a superficial velocity of 407 m/d. The respective filter coefficients are shown next to the fitted relationships. The filter coefficient for coated sand (8.8 m^{-1}) was
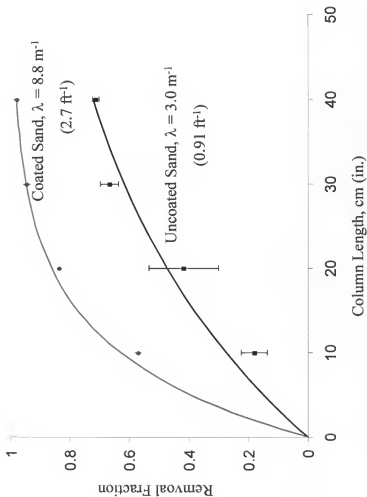
Figure 3-7. Effect of column length on removal of *Cryptosporidium* oocysts in sand filters (Error bars represent ± 1.0 standard deviations. Some error bars are too small to be seen.)

increased by a factor of 2.9 over that of uncoated sand (3.0 m^{-1}). This difference was significant at $P < 0.05$.

The effect of superficial velocity on filter coefficient is shown in Figure 3-8. The range of superficial velocities investigated started at 204 mg/d ($3.5 \text{ gal}/(\text{ft}^2 \text{ min})$), which is typical of rapid sand filters used in municipal water and wastewater treatment facilities. The upper end of the range investigated was 814 m/d ($14 \text{ gal}/(\text{ft min})$), which is on the order of loadings used in high-rate filter systems. The coated sand outperformed uncoated sand over the entire range of superficial velocities tested.

A power law relationship of the form

$$\lambda \propto U^{-\alpha} \tag{3.6}$$

has been suggested to give the effect of superficial velocity on filter coefficient (Wennberg and Sharma, 1997), where U = superficial velocity. This coefficient is critical in determining how sensitive the performance of granular media filters is to superficial velocity. Previous research has indicated that the alpha coefficient is higher in attractive systems than in repulsive systems (Ghosh et al., 1975), which would tend to negate the benefit of coating filter media to achieve a positive zeta potential.

We fit relationship (3-6) to the data in Figure 3-8 by nonlinear least squares regression and show the resulting alpha values on the figure. The alpha value of 0.66 for uncoated sand is within the range of 0.43 to 1 found by Ghosh et al. (1975) for systems with double layer repulsion and high superficial velocities ($U > 86$ m/d). The value of 0.59 for coated sand is well below the alpha of 2 determined by Ghosh et al. (1975) for attractive systems under the same conditions, however. As a check on our results, we computed filter coefficients from data on bacteria removal in columns of coated sand that
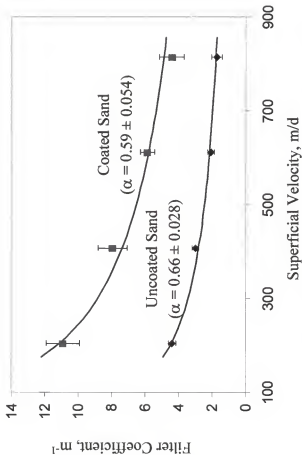
Figure 3-8. Effect of superficial velocity on filter coefficient in sand columns filtering *Cryptosporidium* (L = 40 cm ; Error bars represent ± 1.0 S.D.)

were reported by Ahammed and Chaudhuri (1996). Fits of relationship (4) to these data are given in Figure 3-9. As shown, the values of alpha (0.50 and 0.48) are reasonably close to our results.

This study's average 2.9-fold improvement in filter coefficient for removal of *C. parvum* by coating of sand media with iron/aluminum (hydroxy)oxide is generally better than reported in previous studies on filtration of bacteria or bacteria-sized particles. Ahammed and Chaudhuri (1996) reported λ_c/λ_u of 1.5 to 1.8 for the filtration of heterotrophic bacteria and 1.6 to 2.1 when filtering *Escherichia coli*. At the pH of their experiments (7.8 to 8.1), the bacteria should have carried a negative charge. Stenkamp and Benjamin (1994) found λ_c/λ_u of 1.2 to 2.5 and 1.1 to 1.5, respectively, when filtering negatively charged (at pH 7.0) latexes and ferrihydrite particles. Kang (1998) studied the effect of aluminum and iron hydroxide coatings on fabric filters. He found that the filter coefficients were 2.1-fold greater for coated fabric than uncoated fabric for *Staphylococcus aureus* and 3-fold greater for coated fabric for *Escherichia coli*. No ratios for filtration of protozoa such as *Cryptosporidium* or similarly sized particles is available in the literature. This improvement can be most likely be attributed to the change in zeta potential (from electronegative to electropositive) resulting from the coating process since this would decrease the electrostatic repulsion between the sand and the electronegative *Cryptosporidium* oocysts. Other factors, such as increased surface roughness, may also play a role.
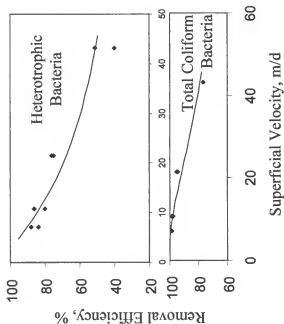
Figure 3-9   Effect of superficial velocity on bacteria removal in sand columns (Ahammed & Chaudhuri, 1996) (L = 15 cm, Sand size = 0.3-0.8 mm)

3-4 Conclusions

Based on the present study, the following conclusions can be drawn:

- A surface coating of hydrous aluminum and iron oxide on Ottawa sand is effective in increasing the zeta potential of the sand from negative values to positive values

- Coated (electropositive) sand significantly improves removals of *Cryptosporidium* oocysts from water at superficial velocities representative of rapid sand filters operated at low to high superficial velocities

- Based on the almost three-fold improvement in filter coefficient, coated sand can significantly increases the reliability of rapid sand filtration systems and prevent breakthrough of *Cryptosporidium* oocysts during periods of suboptimal chemical conditioning

CHAPTER 4
EFFECT OF IRON ALUMINUM (HYDR)OXIDE COATING ON REMOVAL OF *Cryptosporidium* OOCYSTS BY GLASS AND CERAMIC BEADS

4-1 Introduction

Coatings of the oxides and hydroxides (i.e., (hydr)oxides) of iron and aluminum on granular filter media such as sand and diatomaceous earth enhance the filtration of bacteria, viruses, protozoa, and turbidity from water (Ahammed and Chaudhuri, 1996; Chang et al., 1997; Chen et al., 1998; Farrah and Preston, 1991; Gerba et al., 1988; Lukasik et al., 1996; Lukasik et al.,1999; Mills et al., 1994; Shaw et al., 2000; Stenkamp and Benjamin, 1994; Truesdail, 1999). The coatings, which are electropositive, change the zeta potential of the filter media from highly electronegative values to near-zero or positive values. In comparison, microbes and other colloidal particles in water normally carry a negative zeta potential in the natural water pH range of 6 to 8. Improvements in particle removal by coated filter media have thus been attributed to reduction or elimination of electrostatic repulsion between the filter media and colloids (Ahammed and Chaudhuri, 1996; Chang et al., 1997; Chen et al., 1998; Farrah and Preston, 1991; Lukasik et al., 1996; Lukasik et al.,1999; Mills et al., 1994; Shaw et al., 2000; Stenkamp and Benjamin, 1994).

A few investigators have cited other changes to filter media surfaces due to coatings as playing a role in enhanced particle removal. These include surface roughness, surface chemical heterogeneity, surface area, and amphoteric surface charge (Stenkamp and Benjamin, 1994; Sansalone, 1999). Chen et al. (1998) observed, in a long-term

40

wastewater filtration study with aluminum (hydr)oxide coated Ottawa sand, that the zeta potential of the coated sand dropped back to negative values soon after the filters were put into service. However, the coated sand continued to remove significantly more *Escherichia coli* from wastewater than uncoated sand for over 3 months of continuous service.

The present study was carried out to quantify the non-electrostatic contribution of iron aluminum (hydr)oxide coating on granular filter media to removal of *Cryptosporidium* oocysts. Characteristics and performance of glass beads, which have negative zeta potential in the natural water pH range of 6 to 8, were compared to those of coated glass beads, which have positive zeta potential in this pH range. Similarly, characteristics and performance of ceramic beads, which have positive zeta potential in the natural water pH range, were compared to those of coated ceramic beads which also have positive zeta potential in the pH range. The results show that the coating improves filter media performance, even when it has negligible impact on the zeta potential of the filter media.

4-2 Materials and Methods

Chemicals used in this study were purchased from Fisher Scientific unless otherwise indicated.

4-2-1 Filter Media Preparation

Approximately spherical high-silica glass beads (Jaygo Inc., Union, N.J.) and high-alumina ceramic beads (Ferro Corp, Shreeve, Ohio) were used in the study. The glass beads were 72% SiO_2, 9% CaO, 4% MgO, and 1% Al_2O_3 , whereas the ceramic beads were 87% Al_2O_3, 1.4% MgO, 1.4% CaO, 8.7% SiO_2, 0.3% Fe_2O_3, 0.13% TiO_2, 0.4% Na_2O, and 0.4% K_2O, according to the respective manufacturers.

The glass beads had a narrow size distribution, with diameters averaging 0.73 mm. The ceramic beads had a wider size distribution and were sieved to collect the fraction passing a U.S. Standard #25 sieve and retained on a #30 sieve (0.6 to 0.7 mm). The beads were coated with iron aluminum (hydr)oxide according to Shaw et al. (2000). Beads were filled to a depth of 2.5 cm in glass pans and covered with a solution 0.2 M in $FeCl_3 \cdot 6H_2O$ and 0.4 M in $AlCl_3 \cdot 6H_2O$. The solution was immediately drained from the beads and the media were dried at 70°C for 24 h, then cooled to room temperature. Clumps were broken up, beads were added to a beaker containing 4M NH_4OH, and the solution was immediately drained. The beads were spread over flat pans and dried at 70° C for 24 h. After cooling, beads were rinsed with deionized water until the water was clear, air-dried, and finally passed through a #25 sieve. Coated beads were stored in sealed plastic containers until use.

4-2-2 Filter Media Characterization

4-2-2-1 SEM

Beads were carbon-coated (Ion Equipment, Santa Clara, CA) for 1 to 2 minutes to obtain a 100 to 200 Angstrom thick coating and examined by SEM (JSM 6400, thermoionic emission, Tungsten filament). X-ray mapping and quantitative analysis was carried out with an Oxford Instruments Link ISIS EDS System (Oxfordshire, UK).

4-2-2-2 Surface area

Surface areas of beads were measured by five-point BET analysis using krypton adsorbate on a Quantachrome Autosorb-1 (Boynton Beach, FL) physical adsorption analyzer. Approximately 15 grams of beads were placed in a glass sample holder and degassed overnight at 200°C. Three complete multi-point analyses were carried out on

each sample. The correlation coefficient of each BET analysis exceeded 0.99.

4-2-2-3 Zeta potential

Zeta potentials were measured on coating removed in the final rinse of the coating procedure and on the beads before and after coating. Rinse water was passed through Whatman GF/C filters and the filters were dried at room temperature. Dried residue was scraped from the filters and added to aliquots of MilliQ water (Millipore, Bedford, MA) that were previously adjusted to pH values in the range of 3 to 10 using NaOH and HCl. The concentration of coating was approximately 0.03 mg/mL. Each sample was then adjusted to 0.001 M NaCl. The zeta potential of the filter coating was measured on a Brookhaven Zeta Plus (Brookhaven Instruments Corp., Holtsville, NY). The final pH of each aliquot was measured immediately after the zeta potential measurement.

Zeta potential of the beads was determined using an Anton Paar Electro Kinetic Analyzer (EKA, Anton Paar, Graz, Austria). The cylindrical flow cell (2.0 cm I.D.) was packed to a depth of 4.0 cm with glass and ceramic beads. An electrolyte solution (1.0 x 10^{-3} M KCl) was pumped through the flow cell. This caused a charge transfer in the flow direction, resulting in a potential difference (ΔU) that was detected by silver electrodes coated with AgCl, placed at the ends of the cell. A differential pressure sensor was used to measure pressure drop (ΔP) across the cell. The pressure was held at 300 mbar for 2 cycles of 2 minutes each and ΔP and ΔU were recorded. The ratio of these measurements was used to find zeta potential (ζ) according to the Fairbrother and Mastin (1924) equation:

$$\zeta = \left(\frac{\Delta U}{\Delta P}\right)\frac{\eta k}{\varepsilon} \qquad (4.1)$$

where η is the viscosity and k is the conductivity of water. The parameter ϵ in SI units is found from:

$$\epsilon = \epsilon_r \, \epsilon_0 \tag{4.2}$$

where ϵ_r = 78.54 at 25°C and ϵ_0 = 8.85 x 10^{-12} C ^{2} /(J m).

Isolectric points of the coating and beads were determined from quadratic fits of the zeta potential-pH relationships within approximately ± 2.5 pH units, (corresponding to five or more measurements) of the point of zero charge (PZC). The r^2 of each fit was 0.99 or higher.

4-2-2-4 Surface metal content

Acid digestion followed by ICP of digestates was applied to triplicate samples of coated and uncoated beads. A volume of 25.0 mL aqua regia (1:2:2 HCl:HNO_3:H_2O) was added to 10.0 g of oven-dried (105°C) beads and the mixture was boiled for 20 minutes. After cooling, the digestate and water from rinsings of the digestion vial and beads were passed through Whatman GF/C filters and deionized water was added to adjust the final volume to 100 mL. This solution was analyzed for aluminum and iron by ICP.

4-2-3 Performance Testing of Filter Media

4-2-3-1 Batch tests

Aliquots (5.0 g) of beads were placed in triplicate 125 mL Erlenmeyer flasks. A suspension of *Cryptosporidium parvum* (Pleasant Hill Farms, Troy, ID), containing approximately 1000 oocysts per mL, was prepared in artificial ground water (35 mg $MgSO_4 \cdot 7H_2O$, 12 mg $CaSO_4 \cdot 2H_2O$, 12 mg $NaHCO_3$, 6 mg NaCl, 6 mg KNO_3 per litre deionized water; pH 7.0) (McCaulou et al., 1994). A 20 mL volume of this suspension

was added to each flask containing beads, plus three flasks containing no beads (control). The flasks were shaken at 60 rev/min on an orbital shaker table for 60 min. Supernatants were sampled after 5 min. settling. The percent removals of *Cryptosporidium* oocysts were computed based on the mean control concentration vs. the concentrations in the respective flasks containing beads.

4-2-3-2 Column tests

Dry filter media was packed into 1.5 cm I.D. acrylic columns of varying lengths. Glass wool was used at both ends of the columns to prevent loss of filter media. Columns were used in the upflow mode.

Columns containing uncoated beads and coated beads were run in parallel in each trial and were fed artificial groundwater at 20°C. Immediately prior to each experiment, packed columns were rinsed with 70 pore volumes of artificial groundwater at the same flow rate (50 mL/min) used in the experiment. *Cryptosporidium* oocysts were added to 20 to 70 L of artificial groundwater in a plastic container to give approximately 500 to 1000 oocysts/mL. The water was mixed at 60 rev/min with a 5 cm diameter propeller-type impeller throughout the experiments. Influent to the columns was sampled from the container while pore volumes 71 to 75 of the *Cryptosporidium* suspension were entering the columns. Composite effluent samples representing steady-state conditions were collected at the 71st through 75th pore volumes. Shaw et al. (2000) previously determined that pseudo-steady-state conditions were achieved after 10 pore volumes had passed through the column and were maintained for at least 780 pore volumes. Samples were stored at 4°C overnight prior to enumeration. Three trials were carried out for each set of conditions.

The pressure drop in 100 cm long columns of filter media was measured at a flow rate of 50 mL/min (superficial velocity = 407 m/d) using a mercury manometer. The pressure drop due to the filter media was obtained by subtracting the pressure drop through a column without beads from the pressure drop through a column containing beads.

4-2-3-3 Counting of *Cryptosporidium* Oocysts

The procedure for counting *Cryptosporidium* oocysts was based on the fluorescent antibody method of EPA (1995). For each sample, one slide was prepared for the influent and one slide was prepared for the effluent. Reagents used in enumerating *Cryptosporidium* oocysts included phosphate buffered saline (PBS), blocking solution, fluorescent reagent, and mounting medium (Shaw et al., 2000).

Filters were soaked in phosphate-buffered saline (PBS) for 2 min. A wet support filter (0.45 μm effective pore size; Gelman GN6) was placed on each support screen of the vacuum manifold (Hoefer model FH 225V) and a cellulose acetate filter (0.2 μm effective pore size cellulose acetate; Sartorius, Edgewood, N.Y.) was placed atop each support filter. The vacuum was adjusted to 5 to 10 cm Hg, and a manifold valve was opened briefly to flatten the filter. Valves were opened only long enough to drain liquids, in order to avoid drying the filters. The filter was rinsed with 2 mL of blocking solution to limit non-specific background fluorescence. A 5 mL volume of sample was then passed through the filter, followed by an additional rinse of 2 mL of blocking solution. A volume of 0.5 mL fluorescent reagent was placed on the filter and left for 45 minutes. Light was excluded during the contact period by covering the filter funnel with aluminum

foil. After draining the fluorescent reagent, the filter was rinsed 5 times with 2 mL PBS per rinse.

The slide was prepared by placing a 75 µL drop of mounting medium on a slide and warming the slide to 37°C. A single filter was placed atop the mounting medium on a slide, completely wetting the bottom of the filter. A 25 µL drop of mounting medium was added to the top of the filter. Finally, a glass cover slip was placed over the filter and weighted with 5g of coins to flatten the filter. The edges of the cover slip were sealed with quick drying nail enamel.

The 5 to 7 micron diameter *Cryptosporidium* oocysts appeared apple-green and spherical with a darker green outline under epifluoresence illumination (Leitz Microlab with 25x bright field objective and 12x ocular). The entire slide was counted. Since the filtered suspension was in reconstituted water, very little debris was visible on the prepared slides. Typical influent counts per slide were approximately 2000 oocysts, compared to effluent counts of 5 to 800 oocysts.

4-3 Results and Discussion

4-3-1 Characterization of Glass Bead Surfaces

Table 4-1 summarizes the iron and aluminum in coatings relative to surface area of uncoated filter media. This table includes results from previous studies for which measured surface areas of filter media are available. Values of surface metal content (mg metal per g of filter media) and measured surface area (m^2 per g of filter media) were used to compute surface metal ratios (mg metal per m^2 of filter media surface). Media diameters in the table range from 0.6 to 0.85 mm. The surface Fe ratio for glass beads (33.5 mg/m^2) was somewhat higher than the ratio achieved with sand by investigators using similar coating procedure (Lai et al., 2000; Shaw et al., 2000). Benjamin et al.

48

Table 4-1. Surface metal contents of filter media coated with iron or aluminum (hydr)oxides

Media	Diameter (mm)	Surface Area of Uncoated Media (m²/g media)	Surface Fe Content (mg/g media)	Surface Fe Ratio (mg/m²)	Surface Al Content (mg/g media)	Surface Al Ratio (mg/m²)	Reference
Ottawa sand	0.60-0.85	0.04	28	700	--	--	Benjamin et al., 1996
Ottawa sand	0.60-0.85	0.04	25	625	--	--	Chang et al., 1997
Ottawa sand	0.6-0.7	0.1064ᵃ	--	--	0.35	3.3	Chen et al., 1998
Quartz sand	0.85	0.85	5.7	6.7	--	--	Lai et al., 2000
Ottawa sand	0.6-0.7	0.1064	1.25ᶜ	11.7	1.21ᶜ	11.4	Shaw et al., 2000
Glass Beads	0.73	0.009966	0.334ᶜ	33.5	0.178ᶜ	17.9	Present Study
Ceramic Beads	0.6-0.7	0.01413	1.19ᶜ	84.2	(b)	(b)	Present Study

ᵃThe surface area of 0.6-0.7 mm Ottawa sand was measured in the present study

ᵇNot able to measure

ᶜS.D. < 11% of the mean (N=3)

(1996) achieved a considerably higher surface Fe ratio (700 mg/m^2) using a two-step coating procedure in which iron solution [Fe(NO$_3$)$_3$ or FeCl$_3$] was not drained from the sand media prior to the drying step. The surface Al ratio for glass beads (17.9 mg/m^2) was somewhat higher than the ratios achieved by Shaw et al. (2000) and Chen et al. (1998).

Viewed by scanning electron microscopy at 250x, the surfaces of both the coated (Fig. 4-1c) and uncoated (Fig. 4-1a) glass beads appeared relatively smooth, with patches of roughness. Patches on the coated beads were scale-like in appearance (see area in and around the box in the top portion of Figure 4-1c), whereas rough areas on the uncoated bead (e.g., in and around the box in the top portion of Figure 4-1a) had a finer texture. X-ray maps of the uncoated bead (Fig. 4-1b) showed a homogenous distribution of aluminum, iron, and silicon on the surface, including the rough patches, indicating that these patches did not differ from the rest of the surface in their composition. In contrast, the metals were unevenly distributed on the coated bead (Fig. 4-1d). For example, the relative concentration of aluminum and iron was high (lighter colored in the respective Al and Fe maps) in and around the boxed region, whereas in the same area, the relative concentration of silicon was low (darker colored in the Si map). This indicates that the rough, scaly patches on the coated beads were iron aluminum (hydr)oxide coating, which masked the silicon signal from the underlying glass bead surface.

The boxed areas in Figure 4-1 were then examined at 1600x (Fig. 4-2). The differences in texture of these rough patches are clearly evident: on the uncoated bead, this region was characterized by random texture, whereas on the coated bead, it was covered by large flakes of material. Iron, aluminum, and silicon were homogeneously distributed on the uncoated bead (Fig. 4-2b) and unevenly distributed on the coated bead
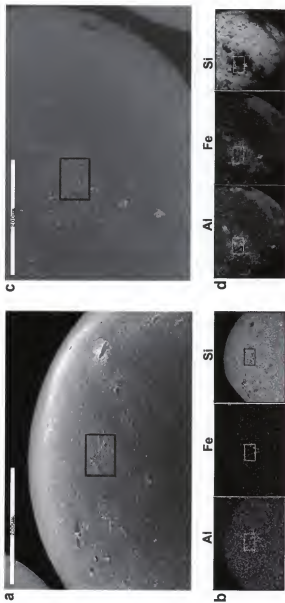
Figure 4-1. SEM images glass beads at 250x; (a) uncoated glass bead, (b) X-ray maps of uncoated glass bead, (c) coated glass bead, (d) X-ray map of coated glass bead. Examples of rough patches are shown in boxes.
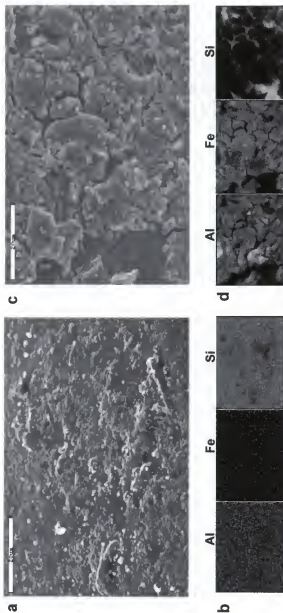
Figure 4-2. SEM images at 1600x of boxed areas in previous figure; (a) uncoated glass bead, (b) X-ray maps of uncoated glass bead, (c) coated glass bead, (d) X-ray map of coated glass bead.

(Fig. 4-2d). Regions of high aluminum and iron concentration on the coated bead corresponded to regions of low silicon concentration and reflected the shapes of the flakes.

Further examinations were carried out at 6000x (Fig. 4-3). The region viewed on each bead was determined by first finding a rough region on the surface, then rotating the sample to show the edge of this region, as well as some foreground area. The foregrounds of coated bead surfaces (Fig. 4-3b, 4-3c) were similar to the uncoated bead surface (Fig. 4-3a) in appearance. Means of duplicate analyses of the foreground in Figure 4-3c gave 1.6 % Al , 1.9 % Fe, and 18 % Si, whereas analyses of the raised region (atop the ledge) in Figure 3c gave higher Al and Fe contents (5.2 % and 9.7 % respectively) and lower Si content (7.2 %). The measurements indicate that the raised region is a flake of iron aluminum (hydr)oxide coating overlying the bead surface. Quantitative X-ray analysis at five different locations on an uncoated bead gave mean elemental compositions of 0.7 % Al , 0.05 % Fe, and 18.0 % Si. The foreground iron and aluminum contents were probably influenced by the proximity of the coating, and thus were somewhat higher than those found on the uncoated bead. The raised region in Figure 4-3b, by its contrasting appearance to the foreground, can also be concluded to represent a flake of coating. The thickness of the flakes is 1 to 2 μm, which is somewhat lower than the 4 to 7 μm thickness reported by Lai et al. (2000) for iron oxide on Ottawa sand.

The surface area of sand within media sizes of 0.6 to 0.85 mm was reported as 0.01 to 0.05 m^2/g by three investigators (Benjamin et al., 1996; Chang et al., 1997; Sansalone, 1999), whereas Lai et al. (2000) gave a surface area of 0.85 m^2/g (Table 4-2). In the present study, we measured areas of 0.11 m^2/g for Ottawa sand and 0.01 m^2/g for
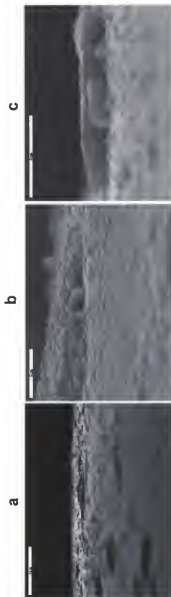
Figure 4-3. SEM image at a plane tangent to the surface of (a) uncoated and (b) coated glass magnified 6000x and (c) coated glass magnified 10,000x.

54

Table 4-2. Effect of coating on surface area of filter media

Media	Diameter (mm)	Surface Area (m²/g)		ΔSA[a]	Surface Fe Ratio (mg/m²)	Reference / Notes
		Uncoated	Coated			
Ottawa Sand	0.60-0.85	0.04	5.8-9.1	7.4	700	Benjamin et al. (1996)
Ottawa Sand	0.60-0.85	0.04	2.7	2.7	625	Chang et al (1997)
Sand	0.67-0.99	0.85	2.76	1.9	6.7	Lai et al (2000)[b]
Silica Sand	0.60-0.80	0.01-0.05	5-15	10	- -	Sansalone (1999)[c]
Ottawa Sand	0.6-0.7	0.106[e]	0.601[e]	0.49	11.7	Present study[d]
Glass Beads	0.6-0.7	0.00997[e]	0.382[e]	0.37	33	Present study[d]
Ceramic Beads	0.6-0.7	0.0141[e]	1.403e	1.4	84	Present study[d]

[a]Change in surface area based on median values

[b]Nitrogen adsorbate

[c]Ethylene glycol monoethyl ether method

[d]Krypton adsorbate

[e]S.D. < 10% of the mean (N=3)

glass beads. Previous studies indicated that coating sand with iron oxide increased the surface area of the media by 1.9 to 10 m^2/g, whereas in the present study the surface area of sand was increased by 0.49 m^2/g and the surface area of glass beads was increased by 0.37 m^2/g. Based on the data shown in Table 4-2, the increase in surface area was significantly correlated with the surface iron ratio ($\alpha = 0.05$).

Chang et al. (1997) suggested that iron oxide coating is highly porous. Coating removed during the rinsing process in the present study had a mean surface area of 285 ± 9.4 m^2/g (N = 3), which is reasonably close to the range of 75 to 108 m^2/g for iron oxide coating (Sansalone, 1999). The particles of coating were irregularly shaped discs, 8 to 50 μm across and 2 to 3 μm thick, with a mean pore diameter of 2.6 nm and total pore volume of 0.19 cm^3/g. The calculated external surface area of the coating particles (approximated as 8 x 2 μm discs to give a high estimate) is 0.46 m^2/g, a value far lower than that measured. Thus, virtually all of the coating surface area must be within its pores. Normalizing the iron content of the glass beads contributed by the coating to the iron content of the coating gives a value of 1.6 mg coating per g glass. Multiplying this value by the surface area of the coating (285 m^2/g) gives 0.45 m^2 of surface area per g glass, which is reasonably close to our measured value of 0.37 m^2/g.

The zeta potential of glass beads, before and after coating with iron aluminum (hydr)oxide, is shown in Figure 4-4. The point-of-zero-charge (PZC) of the uncoated glass beads was 3.7, which is slightly higher than the PZC of 2 to 3 given by Parks (1965) for the alpha-quartz form of SiO_2. Coated glass had a PZC of 8.2, which is consistent with Parks' (1965) value of 7.8 to 9 for aluminum oxides. Using streaming potential technique, Shaw et al. (2000) and Stenkamp and Benjamin (1994) found PZC's of 2.5
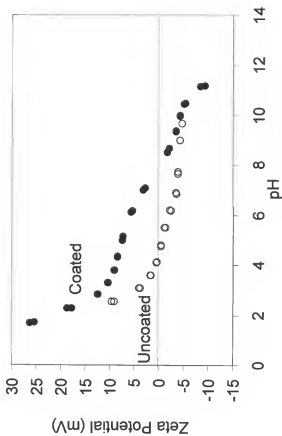
Figure 4-4. Zeta Potential of glass beads, before and after coating with iron aluminum (hydr)oxide

and 3 for uncoated Ottawa sand and 8.0 and 7.5, respectively, for coated Ottawa sand. Using a salt addition technique, Benjamin et al. (1996) and Chang et al. (1997) found a PZC of 0.7 for uncoated Ottawa sand and 9.3 to 9.8 and 10.3, respectively, for iron oxide coated sand.

The zeta potential of the material collected in the final rinsing step of the coating method used in the present study was also measured (Fig. 4-5). The PZC of this material was 8.8, which is somewhat higher than that of the coated glass beads and compares well to PZCs in the range of 8 to 10.3 for iron oxide particles abraded from coated Ottawa sand (Stenkamp and Benjamin, 1994; Chang et al., 1997).

4-3-2 Characterization of Ceramic Bead Surfaces

The textured nature of the ceramic bead surfaces is apparent at 250x (Fig. 4-6). The coated bead (Fig. 4-6c) appears less porous than the uncoated bead (Fig. 4-6a), suggesting that some of the surface texture was filled by the iron aluminum (hydr)oxide coating. X-ray mapping shows homogenous iron distribution on the uncoated bead surface (Fig. 4-6b) and a nonuniform distribution on the coated surface (Fig. 4-6b). At 1600x, a raised mass of material on the bead surface (Fig. 4-7c) corresponds to high-iron regions in the x-ray map. This mass has a scale-like appearance like that seen on the glass beads. The iron distribution on the uncoated bead is uniform (Fig. 4-7b). At 6000x, viewed tangentially, the surface of the uncoated bead appears stringy (Fig. 4-8a), whereas the surface of the coated bead shows cracks and has a "filled in" appearance (Fig. 4-8b).

The surface iron ratio of the coated ceramic beads was 84.2 mg/m^2 (Table 4-1), a value almost three times higher than the ratio for glass beads. The higher amount of iron
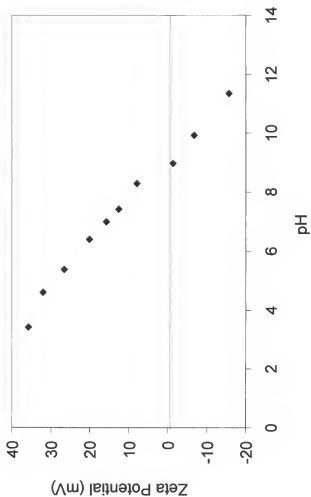
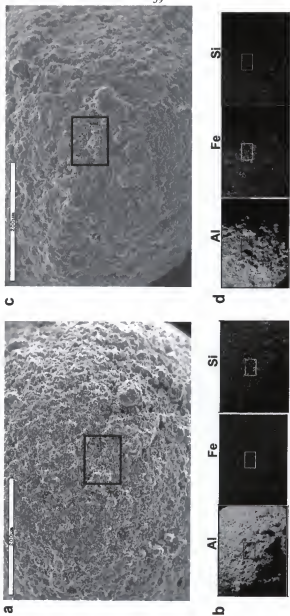Figure 4-5. Zeta Potential of material attrited from the surface of the coated media

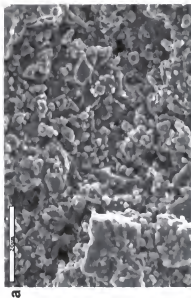Figure 4-6. SEM images ceramic beads at 250x; (a) uncoated ceramic bead, (b) X-ray maps of uncoated ceramic bead, (c) coated ceramic bead, (d) X-ray map of coated ceramic bead. Examples of rough patches are shown in boxes.

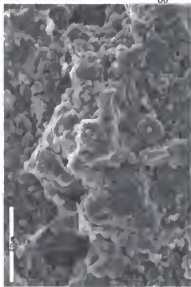Figure 4-7. SEM images at 1600x of boxed areas in previous figure; (a) uncoated ceramic bead, (b) X-ray maps of uncoated ceramic bead, (c) coated ceramic bead, (d) X-ray map of coated ceramic bead.
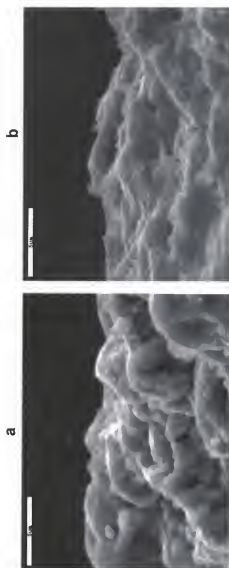
Figure 4-8. SEM image at a plane tangent to the surface of (a) uncoated and (b) coated ceramic magnified 6000x.

on the surface could be a result of the higher surface texture, which can protect coating from attrition during rinsing and handling. Edwards and Benjamin (1989) found that a portion of the iron oxide coating on sand would detach when the sand was subjected to aggressive stirring. The surface area of the ceramic beads was increased from 0.01 m^2/g to 1.4 m^2/g by the coating process, a change that we attribute primarily to porosity of the coating, as discussed previously. Figure 4-9 shows the zeta potential of the ceramic beads. Uncoated ceramic beads had a PZC of 7.9, which is similar to Parks' (1965) value of 7.8 to 9 for aluminum oxides. The PZC was raised to 8.4 by the coating, which is intermediate to the PZC of coated glass (8.2) and the coating material itself (8.8).

4-3-3 Comparison of Filter Media Performance

Batch tests were carried out to avoid column-packing effects and thus provide a direct indication of the interaction between *Cryptosporidium* oocysts and beads (Table 4-3). The tests with glass beads were carried out a pH of 7.0, where the zeta potential of the uncoated beads was negative and the zeta potential of the coated beads was positive. (Fig. 4-4). The uncoated glass beads removed only 5% of the *Cryptosporidium* oocysts from the suspension. The coated beads were significantly ($\alpha = 0.05$) more effective, removing 49% of the oocysts from suspension. Previously, Chen et al. (1998) reported that coating Ottawa sand with aluminum (hydr)oxide increased zeta potential from negative to positive, while improving batch removals of *Escherichia coli* from 10 to 20% to 45 to 60%.

Batch tests with ceramic beads were carried out at a pH of 6.0. At this pH, the zeta potentials of both the uncoated and the coated ceramic beads were positive and nearly identical in magnitude (Fig. 4-9). The uncoated ceramic beads removed 54% of the
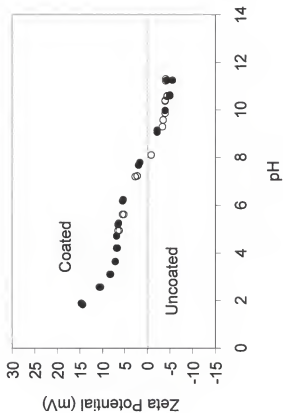
Figure 4-9. Zeta Potential of uncoated and coated ceramic beads (uncoated are open points; coated are filled points)

Table 4-3. Effect of coating on removal of *Cryptosporidium parvum* by glass or ceramic beads in batch tests

	% Removal[a]	
	Uncoated Filter Media	Coated Filter Media
Glass	5.3 ± 3.79	49.3 ± 0.58^b
Ceramic	54.3 ± 1.15	61.3 ± 3.06^b

[a]Mean $\pm$ 1.0 S.D.; N = 3

[b]Significantly higher than uncoated media at $\alpha = 0.05$; N = 3

Cryptosporidium from suspension. Coating the ceramic beads with iron aluminum (hydr)oxide had a negligible effect on their zeta potential, but significantly ($\alpha = 0.05$) improved their performance, increasing *Cryptosporidium* removal to 61%. Continuous-flow column tests were carried out to predict media performance under typical filtration conditions. Porosity of the packed columns of glass and ceramic beads was 39 to 40% (Table 4-4) and was not significantly changed by the coating. The measured pressure drop through a 1.0 m column of uncoated glass beads was 71 mm Hg (superficial velocity = 407 m/d). This agreed closely with the calculated value of 71.3 mm Hg from the Carmen-Kozeny equation (Montgomery, 1985) with a shape factor of 1.0 and temperature of 20°C. Using coated glass beads in the column increased the pressure drop by 7.0%. The measured pressure drop for ceramic beads was 113 mm Hg, which agreed with the Carmen-Kozeny equation with a shape factor of 0.95. Using coated ceramic beads increased the pressure drop by 3.5%.

The change in concentration of particles with respect to column length in a granular media filter may be characterized by the first-order relationship

$$\frac{\partial c}{\partial z} = -\lambda c \tag{4.3}$$

where c is the particle concentration at length z and λ is a coefficient that characterizes the filter media. Integrating this expression gives

$$\frac{c_{effl}}{c_{in}} = e^{-\lambda L} \tag{4.4}$$

which is valid where the coverage of filter media by particles is low enough so that it does not affect the rate of particle attachment. In this expression, c_{in} = influent

Table 4-4. Effect of coating on porosity and pressure drop of 1.0 m long packed columns
(Values given are mean ± 1.0 S.D.; N = 3.)

	Porosity, %		Pressure drop[a], mm Hg	
	Uncoated Media	Coated Media	Uncoated Media	Coated Media
Glass	39.7 ± 0.7	39.4 ± 0.9[b]	71 ± 0.58	76 ± 1.2[c]
Ceramic	40.0 ± 0.3	40.1 ± 1.7[b]	113 ± 2.0	117 ± 2.0[c]

[a]Superficial velocity of water through columns = 407 m/d

[b]Difference between values for coated and uncoated media were not significant at $\alpha = 0.05$

[c]Difference between values for coated and uncoated media were significant at $\alpha = 0.05$

concentration of particles and c_{eff} = effluent concentration of particles. Combining

Equation (4.4) with the definition of fractional removal efficiency ($\eta = 1 - c_{eff}/c_{in}$)

yields

$$\eta = 1 - e^{-\lambda L} \tag{4.5}$$

Equation (4-5) indicates that, as the filter coefficient increases, the removal

efficiency for a given column length also increases.

Figure 4-10 shows least squares nonlinear fits of Equation (4-5) to removal fraction

vs. column length for glass beads at pH 7.0. The filter coefficient for coated glass beads

($5.7\ m^{-1}$) was increased by a factor of 3.0 over that of uncoated glass beads ($1.9\ m^{-1}$). The

difference in filter coefficients was significant at $\alpha = 0.05$. Previously, Shaw et al. (2000)

reported a 2.9-fold increase in filter coefficient using Ottawa sand coated by iron

aluminum (hydr)oxide for removal of *Cryptosporidium* oocysts at pH 7.0. Since the zeta

potential of these coated media at pH 7 is positive, versus negative zeta potential of the

uncoated media, the dramatic improvement in filtration can, at least in part, be attributed

to elimination of electrostatic repulsion between the negatively charged oocysts (at pH 7;

Shaw et al., 2000) and the media.

Figure 4-11 shows fits to removal fraction vs. column length for ceramic beads.

These data were collected at pH 6.0, where the zeta potentials of both the coated and

uncoated ceramic beads were positive and nearly identical in value, whereas the oocysts

had a negative potential (Shaw et al., 2000). The filter coefficient for uncoated beads was

$11.1\ m^{-1}$. Coating the ceramic beads with iron aluminum (hydr)oxide had a significant (α

< 0.05) impact on filter coefficient, increasing it to $19.3\ m^{-1}$ (1.7 x that of the uncoated
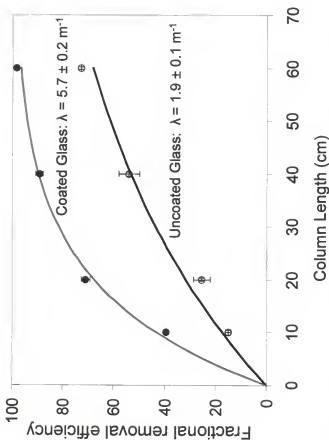
Figure 4-10. Fraction of *Cryptosporidium* oocysts removed at pH 7.0 as a function of column length for uncoated and coated glass beads (Error bars represent mean ± 1.0 S.D for triplicate experiments at each column length. The mean filter coefficients from fits to the three sets of data are shown next to each plot.)
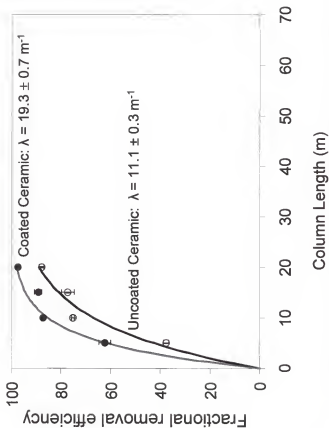
Figure 4-11. Fraction of *Cryptosporidium* oocysts removed at pH 6.0 as a function of column length for uncoated and coated ceramic beads (Error bars represent mean ± 1.0 S.D for triplicate experiments at each column length. The mean filter coefficients from fits to the three sets of data are shown next to each plot.)

ceramic beads). This improvement cannot be attributed to change in zeta potential of the coated vs. uncoated media.

Additional factors contributing to improved *Cryptosporidium* removal by filter media coated with iron aluminum (hydr)oxide coating may include higher surface area available to the oocysts, change in surface roughness, and enhancement of other forces. Most of the surface area increase attributable to coating is present in nanoscale pores, which are too small to admit the oocysts. Nevertheless, deposition of coating in patches, together with its scale-like morphology, should also lead to an increase in the external surface area, resulting in a proportionate increase in capture of oocysts. An increase in external surface area is also consistent with the slightly increased pressure drop resulting from the coatings.

Surface roughness plays a role in interactions between colloids and surfaces, with roughness on appropriate scale significantly increasing favorableness of interactions. However, the coatings applied in the present research did not appear to substantially change the surface roughness of the bead surfaces and, in the case of ceramic beads, may have decreased surface roughness by filling in micron-scale depressions in the bead surface.

Local variations in chemical composition of the surface can produce nonuniform distribution of surface charge and hydrophobicity. Song et al. (1994) have shown, theoretically, that surface chemical heterogeneities can have a profound effect on the attachment rate of negatively-charged colloids onto surfaces with overall negative charge, increasing predicted rates of attachment by orders of magnitude over the predicted rate for a homogenous surface. In the present study, the zeta potential of the coating was slightly higher than that of the ceramic beads, thus, the patchy distribution of coating on

the bead surfaces could affect the distribution of charges on the bead surfaces. However, the effect of positive charge heterogeneity on a surface with overall positive zeta potential has not been investigated. Modification of the hydrophobicity of the media surfaces could also be a factor. Patchy distribution of the hydrophilic (hydr)oxide coating on the ceramic surface might lead to more favorable hydrophobic interactions.

4-4 Conclusions

- In *situ* precipitation of iron aluminum (hydr)oxide on glass and ceramic beads resulted in a patchy distribution of coating on the bead surfaces

- Large increases of BET surface area upon coating filter media with iron aluminum (hydr)oxide coating are largely due to nanoscale pores in the coating

- Pressure drop in packed columns was increased by 4-7% by use of coated media, whereas porosity was unchanged

- Coated glass beads with positive zeta potential were much more effective in removing *Cryptosporidium* from water than uncoated glass beads with negative zeta potential

- Coated ceramic beads with a positive zeta potential removed significantly more *Cryptosporidium* oocysts from water than did uncoated ceramic beads with positive zeta potential

Future research on filter media coatings for enhancing microbe capture should identify characteristics, in addition to zeta potential, that can be enhanced by appropriate coating design. Coating morphology, which affects external surface area and surface roughness, may offer the best possibility for further improving microbe removal in granular media filters.

CHAPTER 5
CONCLUSIONS

The following conclusions can be drawn from this study:

- A surface coating of hydrous aluminum and iron oxide on Ottawa sand is effective in increasing the zeta potential of the sand from negative values to positive values

- Coated (electropositive) sand significantly improves removals of *Cryptosporidium* oocysts from water at superficial velocities representative of rapid sand filters operated at low to high superficial velocities

- Based on the almost three-fold improvement in filter coefficient, coated sand can significantly increases the reliability of rapid sand filtration systems and prevent breakthrough of Cryptosporidium oocysts during periods of suboptimal chemical conditioning

- *In situ* precipitation of iron aluminum (hydr)oxide on glass and ceramic beads resulted in a patchy distribution of coating on the bead surfaces

- Large increases of BET surface area upon coating filter media with iron aluminum (hydr)oxide coating are largely due to nanoscale pores in the coating

- Pressure drop in packed columns was increased by 4 to 7% by use of coated media, whereas porosity was unchanged

- Coated glass beads with positive zeta potential were much more effective in removing *Cryptosporidium* from water than uncoated glass beads with negative zeta potential

- Coated ceramic beads with a positive zeta potential removed significantly more *Cryptosporidium* oocysts from water than did uncoated ceramic beads with positive zeta potential

Future research on filter media coatings for enhancing microbe capture should identify characteristics, in addition to zeta potential, that can be enhanced by appropriate coating design. Coating morphology, which affects external surface area and surface roughness, may offer the best possibility for further improving microbe removal in granular media filters.

CHAPTER 6

REFERENCES

Ahammed, M.M., and Chaudhuri, M. (1996) Sand-based filtration / adsorption media. *J. Water Supply Res. Technol.-Aqua* **45**, 67-71.

Anderson, N.J., Kolarik, L.O., Swinton, E.A., and Weiss, D.E. (1982) Color and turbidity removal with reusable magnetic particles - III. Immobilized metal hydroxide gels. *Water Research*, **16**, 1327-1334.

Angus, K.W., Appleyard, W.T., Menzies, J.D., Campbell, I., and Sherwood, D. (1982) An outbreak of diarrhea associated with cryptosporidiosis in naturally reared lambs. *Veterinary Record* **110**:129.

Benjamin, M.M., Sletten, R.S., Bailey, R.P., and Bennett, T. (1996) Sorption and filtration of metals using iron-oxide coated sand, *Wat. Res.* **30**(11) 2609-2620.

Chang, y., Li, C.-W., and Benjamin, M.M. (1997) Iron oxide-coated media for NOM sorption and particulate filtration. *Journal AWWA.* **89**, 5, 100-112

Chen, J., Truesdail, S., Lu, F., Zhan, G., Belvin, C., Koopman, B., Farrah, S., and Shah, D. (1998) Long-term evaluation of aluminum hydroxide-coated sand for removal of bacteria from wastewater. *Wat. Res.* **32**, 2171-2179.

Considine, R.F., Dixon, D.R., and Drummond, C.J. (2000) Laterally-Resolved Force Microscopy of Biological Microspheres - Oocysts of *Cryptosporidium Parvum*, *Langmuir*, **16**, 1323-1330.

Current, W.L. and Garcia, L.S. (1991) Cryptosporidiosis. *Clin. Micorbiol. Rev.* **4**, 325-358.

Current, W.L., Reese, N.C., Ernst, J.V., Bailey, W.S., Heyman, M.B., and Weinstein, W.M. (1983) Human cryptosporidiosis in immunocompetent and immunodeficient persons. Studies of an outbreak and experimental transmission. *New England Journal of Medicine* **308**, 1252-1257.

Derjaguin, B.V. and Landau, L.D. (1941) Theory of Stability of strongly charged lyophobic sols and the adhesion of strongly charged particles in solutions of electrolyte. *Acta Physiochim.* URSS, **14**, 733.

Dickinson, R.B. (1997) A dynamic model for the attachment of a brownian particle mediated by discrete macromolecular bonds, *Journal of Colloid and Interface Science*, **190**, 142-151.

Dickinson, R.B., Ruta, A.G., and Truesdail, S.E. (2000) Physiochemical basis of bacterial adhesion to biomaterial surfaces in *Anti-microbial / Anti-infective materials: Principles, Applications, and Devices*, Swan, S.P. and Manivannan, G. (eds.), Technomic, Lancaster, PA.

Drozd and Schwartzbrod (1996) Hydrophobic and electrostatic cell surface properties of *Cryptosporidium* oocysts. *Applied and Environmental Microbiology* . **62** (4) 1227.

Edwards, M. and Benjamin, M.M. (1989) Adsorptive filtration using coated sand: a new approach for treatment of metal-bearing wastes. *Journal WPCF*, **61**, 9, 1523-1533.

Elimelech, M., Gregory, J., Jia, X., and Williams, R. (1995) Particle Deposition and aggregation, measurement, modelling, and simulation. Butterworth Heinemann, Oxford.

EPA / 814-B-95-003, ICR Protozoan method for detecting *Giardia* cysts and *Cryptosporidium* oocysts in water by fluorescent antibody procedure, Office of groundwater and drinking water.

Fairbrother, F. and Mastin, H. (1924) Studies in Electro-endosmosis. Part I. *J. Chem. Soc.*, 125, 2319-2330.

Farrah, S. R., and Preston, D. R. (1991). Adsorption of viruses by diatomaceous earth coated with metallic oxides and metallic peroxides. *Wat. Sci. Tech.*, **24**(2), 235-240.

Fayer, R., Graczyk, T.K., Cranfield, M.R., and Trout, J.M. (1996) Gaseous disinfection of *Cryptosporidium parvum* oocysts. *Appl. Environ. Microbiol.*, **62**, 3908-3909.

Fayer, R. and Unger, B. (1986) Cryptosporidium spp. And cryptosporidiosis. *Microbiol. Review*, **50**,458-483.

Fogel, D., Isaac-Renton, J., Guasparini, R., Moorehead, W., and Ongerth, J. (1993) Removing Giardia and Cryptospordium by slow sand filtration. *J. AWWA*. 77-84.

Gerba, C.P., Hou, K., and Sobsey, M.D. (1988) Microbial recovery and inactivation from water by filters containing magnesium peroxide. *J. Environ. Sci. Health*. **A23**, 41-58.

Ghosh, M.M., Jordan, T.A. and Porter, R.L. (1975) Physiochemical Approach to Water and Wastewater Filtration *J. Env. Eng. Div*. 71.

Hamaker, H.C. (1937) The London-van der Waals attraction between spherical particles. *Physica*, **4**, 1058.

Hiemenz, P.C. and Rajagopalan, R. (1997) Principles of Colloid and Surface Chemistry, Third Edition, Marcel Dekker, N.Y., N.Y.

Holly, H.P. Jr. and Dover, C. (1987) Cryptosporidium: a common cause of parasitic diarrhea in otherwise healthy individuals. *Journal of Infectious Disease* **153**:365-368.

Israelachvili, J.N. (1992) Solvation, Structural, and Hydration forces, Intermolecular and Surface Forces, Academic Press, N.Y., N.Y., 260-287.

Kang, P. (1998) Surface Modification of Fibous Filter Media to Enhance Filtration Efficiency, Ph.D. dissertation, Department of Chemical Engineering, University of Florida, Gainesville, FL

Karaman, M.E., Pashley, R.M., Bustamante, H., and Shanker, S.R. (1999) Microelectrophoresis of *Cryptosporidium* oocysts in aqueous solutions of inorganic and surfactant cations. *Colloids and Surfaces A: Physiochemical & Engineering Aspects.* **146,** 217.

Lai, C. H., Lo, S. L., and Lin, C. F. (1994). Evaluating an iron-coated sand for removing copper from water. *Wat. Sci. Tech.* **30**(9), 175-182.

Levine, N.D. (1984) Taxonomy and review of the coccidian genus *Cryptosporidium* (Protozoa, Apicomplexa). *Journal of Protozoology.* **31**, 82.

Liftshitz, E.M. (1956) Theory of molecular attractive forces. *Soviet Physics JETP*, **2**, 73.

Lo, S.-L., Jeng, H.T., and Lai, C.-H. (1997) Characteristics and adsorption properties of iron-coated sand. *Wat. Sci. Tech.* **35**, 63-70.

Long, P.L. (ed.) (1982) The Biology of the Coccidia. University Park Press, Baltimore, MD.

Lukasik, J., Cheng, Y.F., Lu, F., Tamplin, M., and Farrah, S.R. (1999) Removal of microorganisms from water by columns containing sand coated with ferric and aluminum hydroxides. *Water Research*, **33**, 3, 769-777.

Lukasik, J., Farrah, S.R., Treusdail, S., and Shah, D.O. (1996) Adsorption of Microorganisms to sand and diatomaceous earth particles coated with metallic hydroxides. *KONA*, **14**, 1-6.

Marshall, A.R., Al-Jumailli, I.J., Fenwick, G.A., Blint, A.J., and Record, C.O. (1987) Cryptosporidiosis in patients at a large teaching hospital. *Journal Clinical Microbiology* **25**,172-173.

McCaulou , D.R., Bales, R.C., and McCarthy, J.F. (1994) Use of short-pulse experiments to study bacteria transport through porous media. *J. Contam. Hydrol.* **15**,1-14.

Meinhardt, P.L., Casemore, D.P., and Miller, K.B. (1996) Epidemiologic aspect of human Cryptosporidiosis and the role of waterborne transmission. *Epidemilogic Reviews.* **18**(2), 118-136.

Meisel, J.L., Perara, D.R., and Rubin, C.E. (1976) Overwhelming watery diarrhea associated with Cryptosporidium in an immunosuppressed patient. *Gastroenterology* **70**, 1156-1160.

Mills, A.L., Herman, J.S., Hornberger, G.M., and DeJesus, T.H. (1994) Effect of solution ionic strength and iron coatings on mineral grains on the sorption of bacterial cells to quartz sand. *Appl. Environ. Microbiol.* **60**, 3300-3306.

Montgomery, J.M. (1985) Water Treatment Principles and Design, Wiley, New York, New York.

Navin, T.R. and Juranek, D.D. (1984) Cryptosporidiosis: clinical epidemiologic and parasitologic review. *Reviews on Infectious Disease* **6**(B),313-327.

Nime, F.A., Burek, J.D., Page, D.L., Holscher, M.A., and Yardley, J.H. (1976) Acute enterocolitis in a human being infected with the protozoan *Cryptosporidium. Gastroenterology* **70**,592-598.

Ongerth, J.E. and Pecoraro, J.P. (1995) Removing *Cryptosporidium* using Multimedia Filters. *J. AWWA.* December, 1995, 83-89.

Ongerth, J.E. and Pecoraro, J.P. (1996) Electrophoretic mobility of *Cryptosporidium* oocysts and *Giardia* cysts. *J. Environmental Engineering.* 228-231.

Panciera, R.J., Thomassen, R.W. and Garner, F.M. (1971) Cryptosporidial infection in a calf. *Veterinary Pathology* **8**, 479-484.

Parks, G.A. (1965) The isoelectric point of solid oxides, solid hydroxides, and aqueous hydroxo complex systems. *Chem. Rev.* **65**,177.

Rose, J.B. (1998) Occurrence and significance of Cryptosporidium in water. *J. AWWA.* **80**(2), 53-58.

Rose, J.B. (1990) Occurrence and control of Cryptosporidium in Drinking water, Drinking water microbiology : Progress and recent developments, Springer-Verlag, N.Y., 294-321.

Sansalone, J.J. (1999) Adsorptive infiltration of metals in urban drainage - media characteristics. *The Science of the Total Environment*, **235**, 179-188.

Schuler, P.F., Ghosh, M.M., and Gopalan, P. (1991) Slow sand and diatomaceous earth filtration of cysts and other particulates. *Water Research.* **25**, 995-1005.

Shaw, K.M., Walker, S., and Koopman, B. (2000) Improving Filtration of *Cryptosporidium*, *JAWWA*, **92**, 11, 103-111.

Slavin, D. (1955) *Cryptosporidium meleagridis* (sp. nov.) *Journal of Comparative Pathology* **65**, 262-266.

Smith, H.V. and Rose, J.B. (1998) Waterborne cryptosporidiosis: current status. *Parasitology Today*, **14**(1) 14-22.

Song, Lianfa, Johnson, P.R., and Elimelech, M. (1994) Kinetics of Colloidal Deposition onto Heterogeneously Charged Surfaces in Porous Media, *Environ. Sci. Technol.*, **28**, 1164-1171.

Stahl, R. S., and James, B. R. (1991). Zinc sorption by iron-oxide-coated sand as a function of pH. *Soil Sci. Soc. Am. J.*, **55**, 1287-1290.

Stenkamp, S.V. and Benjamin, M.M. (1994) Effect of iron oxide coating on sand filtration. *Journal AWWA* , **86**(8)37-50.

Stenstrom, T.A. (1989) Bacterial hydrophobicity, an overall parameter for the measurement of adhesion potential to soil particles, *Applied and Environmental Microbiology*, **55**, 1, 142-147.

Tilley, M. and Upton, S.J. (1997), In *Cryptosporidium* and cryptosporidiosis; Fayer, R., ed.; CRC Press, Boca Raton, FL, 163-180.

Truesdail, S. (1999) Fundamental Forces Important to the Enhancement of Biological Colloid Removal, Ph.D. Dissertation, Department of Chemical Engineering, University of Florida, Gainesville, Florida.

Tyzzer, E.E. (1910) An extracellular coccidium, *Cryptosporidium muris* (gen. Et sp. nov.), of the gastric glands of the common mouse. Journal of Medical Research **23**:487-516.

Tyzzer, E.E. (1912) *Cryptosporidium parvum* (sp. nov.), a coccidium found in the small intestine of the common mouse. Arch. Protistenkd. **26**:394-412.

Upton, S.J. (1997) In vitro cultivation of Cryptosporidium. In : Cryptosporidiosis of Man and Animals, 2nd ed. Chapter 8, Fayer, R., ed.,CRC Press, Boca Raton, 181-207.

vanLoosdrecht, M.C.M., Lyklema, J., Norde, W., Schraa, G., and Zehnder (1987) Electorphoretic Mobility and Hydrophobicity as a measure to predict the initial steps of bacterial adhesion, *Applied and Environmental Microbiology*, **53**, 8, 1898-1901.

vanLoosdrecht, M.C.M., Lyklema, J., Norde, W., Schraa, G., and Zehnder (1987) The role of bacterial cell wall hydrophobicity in adhesion, *Applied and Environmental Microbiology*, **53**, 8, 1893-1897.

Verwey, E.J.W. and Overbeek, J.T.G. (1948) Theory of the stability of lyophobic colloids, Elsevier, Amsterdam.

Wennberg, K.E. and Sharma, M.M. (1997) Determination of the filtration coefficient and the transition time for water injection wells, Proceedings of the 1997 European formation damage conference (Society of Petroleum Engineers), 353-364

Whitmore, T.N., and Carrington, E.G. (1993) Comparison of Methods for Recovery of Cryptosporidium from water. *Water Science and Technology.* **27**, 69-76.

Woods, K.M. and Upton, S.J. (1998) Efficacy of select antivirals against Cryptosporidium parvum in vitro. FEMS Microbiology Letters **168**,1, 59-63.

Kathryn Shaw was born in Norwood, Massachusetts. She received a Bachelor of Science in Chemistry and Diploma in Engineering from the University of Prince Edward Island, Canada in 1989 and a Master of Science in (Chemical) Engineering from the University of New Brunswick, Canada in 1993. She then returned to the United States to study for a Ph.D. at the University of Florida.

I certify that I have read this study and that in my opinion it conforms to acceptable standards of scholarly presentation and is fully adequate, in scope and quality, as a dissertation for the degree of Doctor of Philosophy.

Ben L. Koopman, Chairman
Professor of
Environmental Engineering Sciences

I certify that I have read this study and that in my opinion it conforms to acceptable standards of scholarly presentation and is fully adequate, in scope and quality, as a dissertation for the degree of Doctor of Philosophy.

Joseph J. Delfino
Professor of
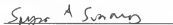Environmental Engineering Sciences

I certify that I have read this study and that in my opinion it conforms to acceptable standards of scholarly presentation and is fully adequate, in scope and quality, as a dissertation for the degree of Doctor of Philosophy.

Hassan E. El-Shall
Associate Professor of
Materials Science and Engineering

I certify that I have read this study and that in my opinion it conforms to acceptable standards of scholarly presentation and is fully adequate, in scope and quality, as a dissertation for the degree of Doctor of Philosophy.

Samuel R. Farrah
Professor of
Microbiology and Cell Science

I certify that I have read this study and that in my opinion it conforms to acceptable standards of scholarly presentation and is fully adequate, in scope and quality, as a dissertation for the degree of Doctor of Philosophy.

Spyros Svoronos
Professor of Chemical Engineering

This dissertation was submitted to the Graduate Faculty of the College of Engineering and to the Graduate School and was accepted as partial fulfillment of the requirements for the Degree of Doctor of Philosophy.

August 2001

Pramod P. Khargonekar
Dean, College of Engineering

Winfred M. Phillips
Dean, Graduate School